

1 **Transferability of machine learning-based modeling frameworks across flood events**
2 **for hindcasting maximum river floodwater depths in coastal watersheds**

Style Definition: Normal (Web)

3 Maryam Pakdehi^{1,2}, Ebrahim Ahmadisharaf^{1,2*}, Behzad Nazari³, Eunsuem Cho^{1,2}

4
5 ¹Department of Civil and Environmental Engineering, FAMU-FSU College of Engineering,
6 Tallahassee, FL 32310

7 ²Resilient Infrastructure and Disaster Response Center, FAMU-FSU College of Engineering,
8 Tallahassee, FL 32310

9 ³Department of Civil Engineering, University of Texas at Arlington, Arlington, TX 76010

10
11 ***Corresponding Author:**

12 Dr. Ebrahim Ahmadisharaf

13 Research Faculty I

14 Department of Civil and Environmental Engineering

15 Resilient Infrastructure and Disaster Response Center

16 FAMU-FSU College of Engineering

17 Tallahassee, FL 32310, USA

18 Tel: +1 716-803-5498

19 Emails: ahmadisharaf@eng.famu.fsu.edu and eascesharif@gmail.com

20 **Abstract**

21 Despite applications of machine learning (ML) models for predicting floods, their transferability
22 for out-of-sample data has not been explored. This paper developed an ML-based model for
23 hindcasting maximum ~~flood~~river water depths during major events in coastal watersheds and
24 evaluated its transferability across other events (out-of-sample). The model considered spatial
25 distribution of influential factors, which explain the underlying physical processes, to hindcast
26 maximum river ~~flood~~water depths. Our model ~~evaluation~~evaluations in a six-digit hydrologic unity
27 code (HUC6) watershed in Northeastern US showed that the model satisfactorily hindcasted
28 maximum ~~flood~~water depths at 116 stream gauges during a major flood event, Hurricane Ida (R^2
29 of 0.9294). The pre-trained, validated model was successfully transferred to three other major
30 flood events, Hurricanes Isaias, Sandy, and Irene ($R^2 > 0.7470$). Our results showed that ML-based
31 models can be transferable for hindcasting maximum river ~~flood~~water depths across events when
32 informed by the spatial distribution of pertinent features, their interactions and underlying physical
33 processes in coastal watersheds.

34 **Keywords**

35 Flood ~~hindcasting~~modeling; Hindcasting; Machine learning algorithms; Maximum flood depth;
36 Model transferability; Coastal watersheds.

37 **1. Introduction**

38 Floods can damage civil infrastructure, business disruptions, and environmental degradation.
39 ~~Nonstationary factors, including land use changes, population growth, and global warming, can~~
40 ~~exacerbate the risk of flood events (Davenport, Burke, and Diffenbaugh 2021; National Academies~~
41 ~~of Sciences, Engineering, and Medicine 2019; Galloway et al. 2018). For instance, (Galloway et~~
42 ~~al. 2018) projected that changes in climate cause a 26.4% increase in the United States flood risks~~

43 ~~by 2050. This increase in flood risk is expected to disproportionately affect poor communities,~~
44 ~~leading to job losses and displacement of residents (Hino and Nance 2021). Therefore, effective~~
45 ~~adaptation and mitigation strategies are urgently needed to maintain resilience against extreme~~
46 ~~future floods (Hemmati et al. 2020; Qi et al. 2021; Wing et al. 2022).~~

47 Mitigation strategies are planned and implemented to mitigate these damages. To propose
48 effective protection strategies, predictive models are used to evaluate watershed responses under
49 various plausible flood scenarios (Fernández-Pato et al. 2016; Kundzewicz et al. 2019; Viglione
50 et al. 2014). These models are essential tools to inform decision makers about suitable risk
51 management strategies and actions. Flood models can be broadly categorized as physically-based,
52 morphologic-based and data-driven.

53 Physically-based models, widely used for predicting hydrologic events, are considered
54 reliable tools for assessing different flood scenarios (Fernández-Pato et al. 2016). These models
55 solve the shallow water equations to derive flood characteristics. Developing physically-based
56 models ~~require~~requires certain meteorologic, hydrologic, and geomorphologic data. If these data
57 are not available at the desired scale, such models cannot be developed. For instance, global
58 inundation models are available to model flooding across the ~~globeworld~~, but they may not be
59 efficient for small scale applications. In such instances, data-driven models can be a flexible
60 alternative as they can adapt to varying levels of data availability by focusing on the features with
61 sufficient data. This flexibility remains one of the advantages of data-driven models over ~~strictly~~
62 ~~data dependent~~—physically-based models. Physically-based models also need significant
63 computational resources, especially in the case of high-resolution, multidimensional (2D and 3D)
64 or stochastic models that necessitate numerous simulations. To enhance the speed of flood
65 simulations, techniques such as parallel computing, graphics processing units (GPUs), and

Field Code Changed

Formatted: Norwegian (Bokmål)

Formatted: Norwegian (Bokmål)

66 simplified models have been utilized (Costabile, Costanzo, and Macchione 2017; Kalyanapu et al.
67 2011; Ming et al. 2020; Sridhar, Ali, and Sample 2021; Zahura et al. 2020). However, resources
68 for utilizing these approaches are not always available (Zhang et al. 2014).

69 Morphologic-based models, which approximate flat-water surfaces over small spatial scales,
70 are also used for flood predictions (Bates 2022). Bathub (Anderson et al. 2018; Kulp & Strauss
71 2019) and height above nearest drainage (HAND; Rennó et al. 2008) are two widely used models
72 in this modeling category. Jafarzadegan and Merwade (2019) used a probabilistic function based
73 on HAND, computed from a digital elevation model (DEM), and optimized it for accuracy, to
74 delineate 100-year floodplains. ~~(Zheng et al. 2018) developed a synthetic rating curve using the
75 HAND method, which accurately represents the river shape and water level measurements, like
76 hydraulic models or stream gauge readings. While these models are computationally efficient, they
77 can overestimate flooded area and are limited to the number of features they use; these models rely
78 on topographic data~~ Zheng et al. (2018) developed a synthetic rating curve using the HAND
79 method, which represents river water depth measurements, similar to hydraulic models or stream
80 gauge readings. While these models are computationally efficient, they can overestimate flooded
81 area and are limited to the number of features they use; these models rely on topographic data
82 (Bates 2022; Bates et al. 2005) and tend ~~only~~ to work well only in confined valleys. The sole use
83 of topographic data makes HAND-based models impractical for low-lying areas, especially coastal
84 watersheds that experience a combination of hydrologic and oceanic processes (e.g., tidal
85 influences, storm surges and wave action); other flood influencing factors, which represent such
86 overlooked underlying physical processes, are needed along ~~forefor~~ predictions in such
87 watersheds. Coastal regions also experience a combination of oceanic and ~~hydrological~~ hydrologic
88 processes, which might not be fully represented by HAND. ~~Additionally, both~~ Both HAND-based

89 and bathtub models are limited in representing such terrains as they might not fully capture the
90 intricate interactions between oceanic and hydrologic factors in coastal areas. Consequently, in
91 coastal watersheds, where unconfined floodplains and complex interactions are prevalent,
92 alternative modeling approaches that consider a broader range of factors are crucial for producing
93 reliable flood predictions. Incorporating these overlooked underlying physical processes becomes
94 essential in providing comprehensive flood predictions in these intricate environments.

95 ~~Machine learning (ML) and, in particular, deep learning (DL) models,~~ offer an alternative
96 approach that can rapidly capture complex relationships between various influencing factors and
97 flood characteristics. ML models have the potential to provide satisfactory flood predictions,
98 ~~making them a valuable tool for improving flood prediction accuracy~~ (Mishra et al. 2022). Such
99 data-driven models have gained popularity in overcoming the limitations of physically-based and
100 morphologic-based models in flood ~~analyses~~modeling (Khosravi et al. 2018). These models
101 mathematically represent the nonlinearity of flood dynamics using~~with~~ pertinent features and
102 observed flood data, ~~and through their intricate~~ using complex nonlinear structures and algorithms.
103 Data-driven models have been found as promising tools due to their quick development time and
104 minimal input requirements (Guo et al. 2021; Löwe et al. 2021; Zahura et al. 2020); ~~therefore, they~~
105 ~~are effective for short-term forecasts and nowcasts (Mosavi, Ozturk, and Chau 2018). ML and DL~~
106 ~~models can discover and leverage hidden patterns within the data, leading to improved~~
107 ~~performance as the amount of available data increases. By recognizing and utilizing these~~
108 ~~underlying patterns inherent in the data, ML and DL models can make satisfactory predictions (in~~
109 ~~terms of minimum error in estimating flood characteristics like depth) and generate valuable~~
110 ~~insights. Example data-driven models for flood prediction include multi-criteria decision-making~~
111 ~~techniques, multiple linear regression, artificial neural networks (ANNs), random forest,~~

112 ~~convolutional neural networks, support vector machine, support vector regression, frequency ratio~~
113 ~~models, and weights of evidence models (Adamowski et al. 2011; Kim et al. 2016; Rafiei-Sardooi~~
114 ~~et al. 2021; Rahmati et al. 2016; Rezaie et al. 2022; Wang et al. 2015; Youssef et al. 2022).~~

115 . Example data-driven models for flood predictions include multiple linear regression, artificial
116 neural networks (ANNs), random forest, support vector machine, and support vector regression
117 models (Adamowski et al. 2011; Kim et al. 2016; Rafiei-Sardooi et al. 2021; Rahmati et al. 2016;
118 Rezaie et al. 2022; Wang et al. 2015; Youssef et al. 2022). While there are several issues with
119 these models, including interpretability, techniques such as SHapley Additive exPlanations
120 (SHAP) can enhance understanding of these models' decision-making processes (Lundberg and
121 Lee 2017; Abdollahi and Pradhan 2021). These models enable the identification of key features
122 that drive flood characteristics.

123 Previous research has shown that various ML algorithms are effective in predicting flood
124 extents and generating susceptibility maps, with a focus on classification ML models (Khosravi et
125 al. 2018; Rahmati et al. 2016; Rezaie et al. 2022; Youssef et al. 2022). However, these studies ~~may~~
126 have limitations in terms of their experimental design and scope. For instance, some of these
127 studies created ~~simplified~~ datasets of flooded and unflooded points using remote sensing. The
128 datasets were often split into ~~training and validation data, and different ML models were examined~~
129 ~~on the same dataset.~~ two subsets, and ML models were examined trained on a portion of the dataset
130 (training set) and then tested for the remainder of the dataset (validation or test set). This approach
131 helps in identifying the most effective models for flood predictions based on performance metrics,
132 such as recall or the area under the Receiver Operating Characteristic (ROC) curve. Another
133 limitation of these ML studies is the reliance on a single event for training and validation. As such,
134 it is unclear whether a trained and validated model can satisfactorily predict other flood events.

Field Code Changed

Formatted: Norwegian (Bokmål)

Formatted: Norwegian (Bokmål)

135 These limitations call for studies that evaluate more complex methodologies and a broader range
136 of scenarios on the effectiveness of ML algorithms for predicting flood characteristics. These
137 limitations call for studies that evaluate more complex methodologies and a broader range of
138 scenarios on the effectiveness of ML algorithms for predicting flood characteristics.

139 Another application of ML models for flood inundation prediction has been
140 ~~incorporating~~coupling them with physically-based models for improving their performance. Such
141 applications are based on the hybrid use of ML and physically-based modeling categories. For
142 instance, Chang et al. (2022) suggested an approach that incorporated principal component
143 analysis, ~~(PCA)~~, self-organizing maps, and nonlinear autoregressive models with exogenous inputs
144 to mine spatiotemporal data and forecast regional flood inundation. ~~They~~The authors recognized
145 the value of using ML algorithms ~~in conjunction~~together with a 2D hydraulic model to simulate
146 urban flood inundation ~~while taking~~considering different rainfall ~~occurrences into account~~events.
147 Elkhrachy (2022) developed a hybrid approach to predict flash flood depths combining 2D
148 hydraulic modeling with ML algorithms; water depths simulated by the Hydrologic Engineering
149 Center's River Analysis System (HEC-RAS; Brunner 2016) model served as ~~inputs to~~training and
150 test datasets for ML algorithms. Löwe et al. (2021) trained an ANN model to identify patterns in
151 rainfall hyetographs and topographic data to enable fast predictions of flood depths for ~~new~~
152 ~~rain~~other rainfall events and locations (out of training sample data) complemented by 2D
153 hydrodynamic simulations. Guo et al. (2021) used a convolutional neural network (CNN) model
154 trained on flood simulation patch data from the CADDIES cellular-automata model to perform
155 image-to-image translation for rapid urban flood prediction and risk assessment. To ~~effectively~~
156 simulate maximum flood extent and depth, Hosseiny et al. (2020) created a system that combines
157 a hydraulic model with ML algorithms. Zahura et al. (2020) used simulations from high-resolution

158 1D/2D physically-based models as training and test data for a random forest model that included
159 topographic and environmental characteristics to estimate hourly water depths. In these
160 applications, flood depth, which is important for risk assessments and damage estimates (Merz et
161 al. 2010), has been predicted by coupling physically-based and ML models. These coupled
162 modeling studies demonstrated the complimentary benefits of physically-based models along with
163 ML algorithms in producing flood modeling outputs, but the computational expense is still an
164 application barrier. Another significant challenge inherent in these studies lies in their dependence
165 on ~~2D~~hydraulic models for training purposes. Furthermore, there ~~appears to be~~ a gap in
166 demonstrating the ability of these studies to successfully predict ~~outcomes~~flood characteristics
167 beyond their training samples. For instance, ~~we are unaware of~~no studies ~~that convincingly~~
168 ~~exhibit~~have explored the capability of ML models to predict events ~~of greater magnitude~~other
169 than those utilized in their original training datasets- (out-of-sample).

170 ~~Despite previous efforts, the development of computationally efficient and user-friendly flood~~
171 ~~prediction models remains a challenge. ML-based models, although promising and~~
172 ~~computationally efficient, have not gained widespread acceptance among practitioners due to~~
173 ~~concerns about their reliance on predicting flood characteristics for other events (out of sample).~~
174 ~~While some studies have demonstrated promising results in generating flood hazard maps by~~
175 ~~applying models to new geographical areas not used for training (Bentivoglio et al. 2022; Kratzert~~
176 ~~et al. 2019; Zhao et al. 2021), few studies have examined the transferability of coupled ML and~~
177 ~~physically-based models for predicting flood depths by applying them to unseen data not used in~~
178 ~~training (Guo et al. 2021; Löwe et al. 2021). It, therefore, remains unclear whether an ML-based~~
179 ~~model, which is trained, validated, and tested against a historical event, performs satisfactorily in~~
180 ~~predicting flood characteristics of other events in the same watershed. Floods originate from~~

181 various sources, especially in coastal areas, where flooding heavily relies on the unique
182 characteristics of storm events. High wind events tend to generate storm surges that move
183 upstream, while intense rainfall over upstream watersheds leads to fluvial flooding that moves
184 downstream towards the coast. Conversely, slow moving storm systems can cause intense local
185 rainfall, resulting in overland runoff entering rivers along their paths rather than a concentrated
186 upstream inflow flood wave. Hence, it is crucial to avoid overfitting an ML model to a single
187 historical flood event, as it can lead to significant underperformance in handling other events.

188 A further limitation of past research is the sole focus on predicting greatest flood extents using
189 classification-based algorithms, while the performance of regression-based ML models for
190 predicting other important characteristics like flood depths has not been investigated. Additionally,
191 the importance of spatial distribution of input features has been overlooked in past ML-based flood
192 modeling. To hindcast a flood characteristic at a given location, the features have been
193 incorporated at that location, but flooding is generated through contributions by several other
194 factors that are relevant across the upstream contributing watershed (in inland systems) and/or
195 from the downstream coastline (in coastal systems). The investigation of these research gaps
196 highlighted above is crucial to improve our capability in reliably hindcasting maximum flood
197 depths using computationally efficient and easy-to-use modeling frameworks.

198 Despite previous efforts, the development of computationally efficient and user-friendly flood
199 prediction models remains a challenge. ML-based models, although promising and
200 computationally efficient, have not gained widespread acceptance among practitioners due to
201 concerns about their reliance on predicting flood characteristics for other events (out-of-sample).
202 Transferability is particularly crucial given the growing reliance on ML modeling methods, like
203 ANNs, as suggested by Wenger and Olden (2012). The term "transferability" refers to the model's

204 ability to predict different flood events beyond the scope of its training data, validating its
205 applicability to unseen scenarios, potentially with their unique characteristics (Jiang et al. 2024;
206 Wagenaar et al. 2018). Furthermore, there has yet to be research investigating the extent to which
207 flood depths prediction models can be transferred and applied successfully to different events
208 beyond the initial training settings. It, therefore, remains unclear whether an ML-based model,
209 which is trained, validated, and tested against a historical event, performs satisfactorily in
210 predicting flood characteristics of other events in the same watershed. Floods originate from
211 various sources and the flood characteristics depend on the unique characteristics of storm events.
212 High wind events tend to generate storm surges that move upstream, while intense rainfall over
213 upstream watersheds leads to fluvial flooding that moves downstream towards the coast.
214 Conversely, slow-moving storm systems can cause intense local rainfall, resulting in overland
215 runoff entering rivers along their paths rather than a concentrated upstream inflow flood wave.
216 Hence, it is crucial to avoid overfitting an ML model to a single historical flood event, as it can
217 lead to significant underperformance in handling other events.

218 A further limitation of past research is the sole focus on predicting greatest flood extents using
219 classification-based algorithms, while the performance of regression-based ML models for
220 predicting other important characteristics like flood depths has not been investigated. Additionally,
221 the importance of spatial distribution of input features has been overlooked in past ML-based flood
222 modeling. To hindcast a flood characteristic at a given location, the features have been
223 incorporated at that location, but flooding is generated through contributions by several other
224 factors that are relevant across the upstream contributing watershed (in inland systems) and/or
225 from the downstream coastline (in coastal systems).

226 This paper aimed to fill ~~these~~the abovementioned research gaps by examining the performance
227 and transferability of ML models in hindcasting maximum ~~flood~~water depths across various events
228 in a coastal watershed. Our objective was to develop a transferable, computationally efficient
229 model to hindcast maximum water depths. We aim to evaluate the performance of ML models,
230 which are trained and tested based on an event, and shed insights on the application of the model
231 for predicting maximum river flood depths. ~~To achieve this, the~~ for other events as well. Our study
232 developed a modeling framework based on an ML algorithm. ~~The developed ML-based model~~
233 ~~combined the~~ Multi-Layer Perceptron (MLP) architecture for our ANN model. This algorithm
234 was coupled with feature selection methods and geospatial data. We evaluated the performance of
235 this model against one extreme flood event, Hurricane Ida, across a coastal watershed (six-digit
236 hydrologic unity code [HUC6])—Lower Hudson—in Northeastern US. Next, we assessed the
237 transferability of our developed model across three other extreme events—Hurricanes Isaias,
238 Sandy, and Irene—in the same watershed. These events encompass varied rainfall intensities, wind
239 speeds and storm track directions. Unlike past ML-based modeling studies, which focused solely
240 on predicting flood status (flooded or unflooded), our regression-based model estimates maximum
241 ~~flood~~water depths. This model was also examined against multiple events, more than one single
242 event that has been the focus of past research (~~Bafitlhile and Li 2019; Dawson et al. 2006; Hosseini~~
243 ~~et al. 2020). The model also considered the spatial dimension for predicting flood. The model also~~
244 considered the spatial dimension for predicting maximum water depths at a given location, in
245 which the features were represented either at that location or across the contributing watershed.
246 This ML model is generic and can be applied to hindcast ~~flood~~maximum water depths at non-
247 gauge river sites to get a denser reconstruction of an event along the river network and hindcast

248 water ~~levels~~depths in watersheds with similar drainage area (HUC6 or larger) and flood type
249 (fluvial and coastal).

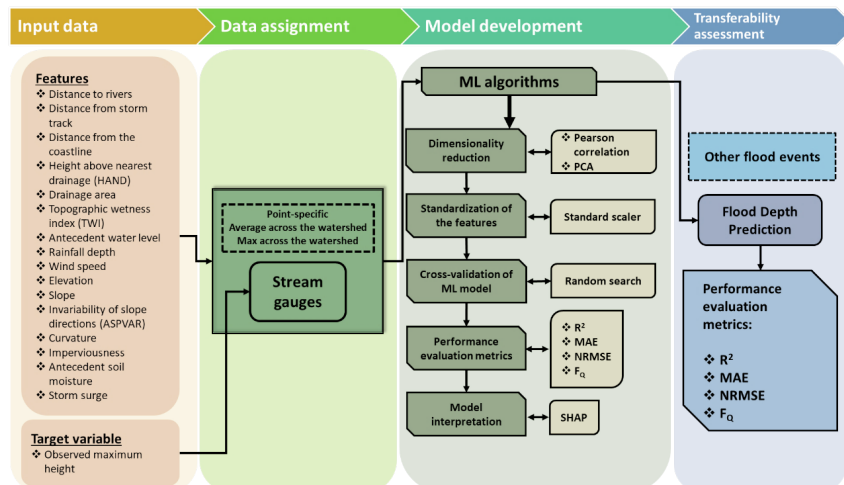
250

251 2. Methodology

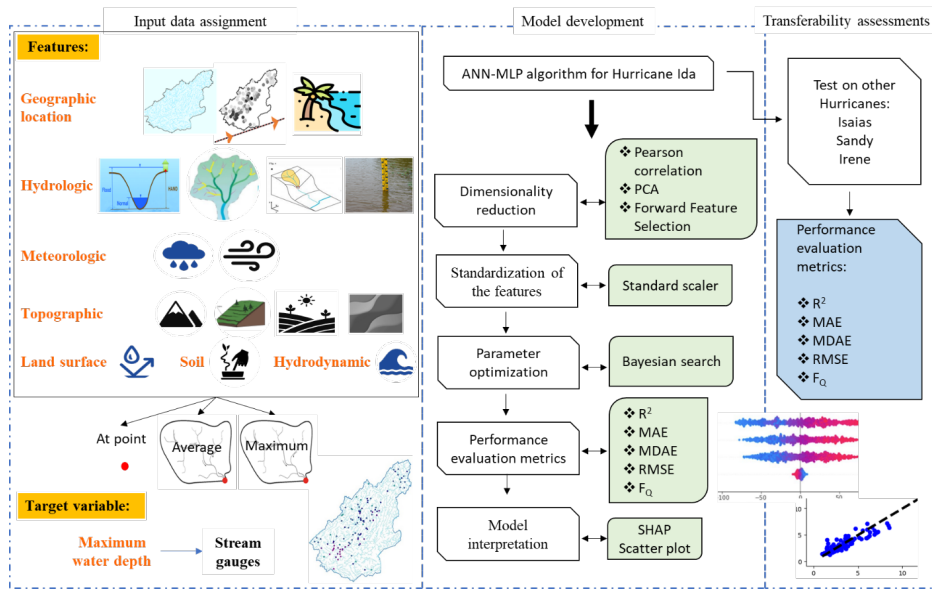
252 We developed an ML-based model that ~~hindeast~~hindcasts maximum ~~flood~~water depths at
253 stream gauges across a coastal watershed during ~~ana~~ flood event (Figure 1). A coastal watershed
254 receives flood contributions from the inland and coastal systems (~~i.e.g.~~, fluvial, and tidal). The
255 model uses geospatial analyses and ML algorithms to hindcast maximum ~~flood~~water depths during
256 an event at river cross-sections of a given watershed. This model is informed by the underlying
257 physical flood processes represented by a wide array of features (topographic, meteorologic,
258 hydrologic, land surface, soil and hydrodynamic).

259 Geospatial operations were conducted to compute the features at stream gauges and/or over their
260 contributing watersheds (the upstream area that drains water to the gauge) ~~with a careful~~
261 ~~consideration of~~considering the underlying physical processes. We used feature selection
262 techniques to determine the most key features ~~and used those infor~~ our ML model. Applying
263 observed data from stream gauges during a flood event, the model was trained, cross-validated,
264 and tested. We then evaluated the model transferability by examining its performance in three
265 other extreme flood events.

Formatted: Indent: First line: 0"



266



267

268

269

270

Figure 1. Schematic view of the machine learning (ML)-based model for hindcasting maximum floodwater depths in coastal watersheds. ANN: Artificial neural network; PCA:

Principal component analysis; SHAP: Shapley additive explanations; MAE: Mean absolute error;

Formatted: Caption, Left

271 ~~NRMSE: Normalized root mean square~~MAE: Median absolute error; F_Q: ~~ratio~~Ratio of
272 estimated over observed maximum flood depth.

273 2.1. Selection and calculation of key features

274 ~~When developing an ML model, the features play a pivotal role in determining its performance~~
275 ~~and estimation capability. By selecting the most relevant and representative features, we empower~~
276 ~~the model to discern the underlying patterns and relationships within the data more accurately. The~~
277 ~~ultimate objective is to enable the model to comprehend the complexities associated with flooding,~~
278 ~~a phenomenon influenced by a myriad of interrelated factors. For an ML estimation accuracy to~~
279 ~~be transferable~~To develop a transferable ML model for complex physical phenomena of flooding,
280 the selection process should extend beyond merely choosing features based on their individual
281 statistical significance. Instead, it should focus on identifying features that collectively contribute
282 to a holistic representation of the phenomenon. ~~This approach ensures that the ML model can~~
283 ~~generalize well to unseen data and handle various real-world scenarios effectively. By~~
284 ~~incorporating this comprehensive set of features, the ML model can capture the nuanced~~
285 ~~interactions between these features; this enhances the model estimation performance.~~

286 We selected key features for our ML-based flood model according to the ~~existing~~past research
287 and the underlying physical processes. Our model considers these features from five broad
288 categories of geographic location, hydrologic, topographic, land surface, soil, and hydrodynamic
289 (Table 1). Here, we provide information on how to derive the features to hindcast ~~flood~~maximum
290 ~~water~~ depths during a flood event in a coastal watershed. Aside from the soil category that
291 represents pre-flood conditions (antecedent soil moisture), all other features represent conditions
292 during a flood event.

294

295 Table 1. Machine learning model features and the assignment approaches for stream gauges.

Formatted: Caption, Left, Keep with next

Category	Feature	Point-specific	Spatial average across the contributing watershed	Spatial maximum across the contributing watershed
Geographic location	Distance to rivers		*	
	Distance from storm track	*		
	Distance from the coastline	*		
Hydrologic	Height above nearest drainage (HAND)		*	
	Drainage area	*		
	Flow accumulation	*		
	Topographic wetness index (TWI)	*	*	
	Antecedent/Initial water level/depth	*		
Meteorologic	Rainfall depth	*	*	*
	Wind speed	*	*	*
Topographic	Elevation	*		
	Ground slope	*	*	
	Slope aspect	*	*	
	Slope aspect invariability (ASPVAR)		*	
	Curvature	*	*	
Land surface	Imperviousness		*	
Soil	Antecedent soil moisture	*	*	
Hydrodynamic	Storm surge	*	*	

296

297 By integrating all these factors into our methodology, we developed a flood hindcast model
 298 that ~~accounts for~~ considers key processes in a coastal ~~watershed~~ watersheds. We used a two-step
 299 process to assign feature values to a point located on a stream gauge. Depending on the feature,
 300 we assigned specified values to the gauge itself or its contributing watershed to consider the spatial
 301 dimension in flood generation processes. For the contributing watershed, spatial mean, and
 302 maximum across the contributing watershed of a given stream gauge was computed. This method
 303 ensures that the feature values indicate the overall pertinent physical processes occurring at the
 304 streams and upstream watersheds. Table 1 specifies how each feature was used in our model.

305 For features under the geographic location category, we incorporated distance to rivers—a
306 critical factor in determining flood ~~risk in numerous studies~~risks (Cao et al. 2020; Rafiei-Sardooi
307 et al. 2021), storm track—specific to the flood event from (National Hurricane Center 2022)—and
308 distance to the nearest coastline. The proximity of a location to waterbodies, such as rivers or
309 coastlines, directly influences its vulnerability to flooding. Coastal regions are susceptible to storm
310 surges, which occur during tropical storms or hurricanes. Storm surges are massive walls of
311 seawater that get pushed ashore by intense winds. ~~As a result, coastal areas can experience severe~~
312 ~~flooding.~~Storm tracks, ~~however,~~ are pathways in the atmosphere along which storms, ~~such as (e.g.,~~
313 ~~hurricanes, tropical cyclones, or extratropical storms.)~~ tend to move. These storms often carry
314 heavy rainfall, intense winds, and storm surges, which can lead to severe flooding in areas they
315 pass over or affect. The distance to storm track and coastline is both considered “Point-
316 ~~specific~~based” as they are specific to individual locations. However, distance to rivers is identical
317 (zero) at these stream gauges, but different in the contributing watersheds, ~~so,~~ we calculated the
318 spatial average distance of the contributing watersheds to the rivers.

319 Under the hydrologic category, we employed four variables of HAND, drainage area, flow
320 accumulation, topographic wetness index (TWI), and ~~antecedent~~initial water ~~level~~depth. HAND
321 represents the elevation of a location relative to the nearest stream. This feature is widely used in
322 flood modeling due to its ability to hindcast flood-prone areas by considering topography and
323 ~~water~~ flow characteristics (Hu and Demir 2021). As its value at the stream gauges is zero, its spatial
324 average across the contributing watershed was considered. The drainage area provides information
325 about potential runoff, while flow accumulation feature helps predict ~~water~~ flow paths during flood
326 events that is previously used by Löwe et al. (2021) and Pham et al. (2021). Both drainage area
327 and flow accumulation values at point of stream gauge (Point-~~specific~~) ~~were captured.~~ TWI was

328 ~~calculated using Equation (1) based on the ground slope and drainage area of the contributing~~
329 ~~watershed (Beven and Kirkby, 1979), and based) were captured. TWI was used by (Gudiyangada~~
330 ~~Nachappa et al. 2020; Löwe et al. 2021; Pham et al. 2021; Zahura et al. 2020; Zhao et al.~~
331 ~~2020)(Gudiyangada Nachappa et al. 2020; Löwe et al. 2021; Pham et al. 2021; Zahura et al. 2020;~~
332 ~~Zhao et al. 2020) and calculated using Equation (1) (Beven and Kirkby, 1979).~~

$$TWI = \ln\left(\frac{\alpha}{\tan(\beta)}\right) \quad (1)$$

334 where, α is the ~~upslopeslope of the~~ contributing ~~areawatershed~~ per unit contour length (as known
335 as the specific catchment area), and β is the local slope gradient in radians. ~~Its~~The TWI value was
336 considered ~~for both "Point specific"point-based~~ and "spatial average across the contributing
337 watershed" to represent the specific location and the overall characteristics of the contributing
338 watershed. The last feature in this category ~~is antecedentwas initial~~ water ~~leveldepth~~, which refers
339 to the ~~stream~~ gauge height one day before the event ~~as; this feature~~ was considered ~~"Point specific"~~
340 ~~for stream gaugespoint-based and explains initial conditions in the study rivers.~~

341 The meteorologic category features were precipitation (Rafiei-Sardooi et al. 2021) and wind
342 speed. Rainfall is the main driving force for floods (Mishra et al. 2022). Storms can bring intense
343 and prolonged ~~rainfallprecipitation~~ to certain areas. If a storm passes over or near a location, it can
344 result in excessive precipitation, overwhelming local drainage systems and causing flooding in
345 low-lying or poorly drained areas. Wind speed is another ~~key~~ feature that can influence the severity
346 and extent of flooding, especially ~~in the context ofduring~~ hurricanes. Intense winds during storms
347 and hurricanes generate large and powerful waves in the ocean. These waves can exacerbate the
348 impact of storm surges, causing even more coastal flooding as they crash onto the shore and flood
349 areas even farther inland. We obtained daily precipitation and wind speed data for the entire period

350 of flood event from weather stations of the National Oceanic and Atmospheric Administration
351 National Centers for Environmental Information (NOAA's NCEI 2022). Their maximum values
352 over a flood event were computed at each stationstream gauge. Using point-based precipitation
353 and wind speed data, we then created a spatially distributed rainfall and wind speed dataset by
354 interpolating the maximum values using the Inverse Distance Weighting (IDW) method (Hosseini
355 et al. 2020). Rainfall depth and wind speed are considered for "Point-specific," "point-based,
356 spatial average across the contributing watershed," and "spatial maximum across the contributing
357 watershed." These values capture the intensity of the ~~meteorological~~meteorologic conditions at
358 individual points and the overall average and maximum values across the upstream watershed.

359 Elevation, ground slope, slope aspect, aspect invariability (ASPVAR), and curvature were
360 features under the topographic category (~~Cao et al. 2020; Chen et al. 2023; Huang et al. 2022;~~
361 ~~Khosravi et al. 2018; Rafiei-Sardooi et al. 2021; Sun et al. 2020~~); (Cao et al. 2020; Chen et al. 2023;
362 Huang et al. 2022; Khosravi et al. 2018; Rafiei-Sardooi et al. 2021; Sun et al. 2020; Fereshthepour
363 et al. 2024), DEM with a resolution of 1/3 arc-second (~10 m) was acquired from the United States
364 Geological Survey (USGS 2022), National Elevation Dataset (NED). To remove any ~~fakespurious~~
365 depressions, the DEM sinks were filled. ~~Before beginning any hydrological study with DEM data,~~
366 this is a suggested step to account for artificial depressions that is frequently employed
367 can impede
368 the realistic simulation of water flow, ensuring that the derived water pathways and other
369 hydrologic computations reflect true surface conditions (~~Khosravi et al. 2018; D. Zhu et al.~~
370 ~~2013~~); (Khosravi et al. 2018; Zhu et al. 2013). Elevation, ground slope, slope aspect, invariability
371 of slope directions (ASPVAR), and curvature ~~all~~ were all derived from the DEM. Elevation allows
372 us to identify low-lying regions prone to floods and hindcast the flood-maximum water depths.
Ground slope is ~~one of the most~~ key ~~factors~~factor in driving water movement. The ground slope

Formatted: Norwegian (Bokmål)

373 ~~of the land, also known as the topography or gradient,~~ plays a crucial role in determining the
374 direction and velocity at which water flows across the landscape. On sloped ~~terrain~~terrains, water
375 flows along the path of least resistance, ~~which is typically downhill.~~ The slope ~~angle of the slope~~
376 determines the speed and volume of surface runoff, influencing the potential for flooding. Slope
377 aspect provides insights into surface runoff distribution and flow ~~concentration~~accumulation by
378 indicating the direction ~~that each of the ground~~ slope faces~~that~~ affects hydrologic processes
379 (Gudiyangada Nachappa et al. 2020; Rafiei-Sardooi et al. 2021). Similar to ~~(Gudiyangada~~
380 ~~Nachappa et al. 2020), we divided~~Gudiyangada Nachappa et al. (2020), we divided the slope aspect
381 into 10 categories: north (0°-22.5°; 337.5°-360°), northeast (22.5°-67.5°), east (67.5°-112.5°),
382 southeast (112.5°-157.5°), south (157.5°-202.5°), southwest (202.5°-247.5°), west (247.5°-
383 292.5°), northwest (292.5°-337.5°), and flat (0°). ASPVAR values near zero indicate diverse
384 catchment watershed slope aspects, while values approaching 1.0 imply a dominant direction (Wan
385 Jaafar and Han, 2012). This feature provided information about surface runoff distribution and
386 flow concentration by specifying the direction that water would flow across the terrain (Dawson
387 et al. 2006). Additionally, analyzing the curvature helped us understand how it impacts flood
388 events, ~~as the topographic curvature plays a role in determining the flow of runoff~~ (Khosravi et al.
389 2018; Pradhan 2009). Elevation ~~is was~~ considered "Point specific"; point-based, while ground
390 slope, and curvature ~~are were~~ considered for both "Point specific"; point-based and "spatial average"
391 across the contributing watershed," indicating how these topographic features vary throughout the
392 entire watershed. ASPVAR conceptually represents the "spatial average across the contributing
393 watershed," capturing the overall characteristics of watersheds.

394 The land surface category was represented by only one variable, imperviousness. ~~On~~
395 ~~impervious surfaces, that reduce~~The greater the ~~ability of soil to absorb rainfall via infiltration,~~

396 ~~imperviousness, the larger volumes~~the volume of surface runoff ~~are produced and propagated~~
397 ~~downstream. In fact, impervious.~~ Impervious surfaces increase both ~~the quantity~~volume and
398 velocity of runoff, ~~and this is~~ due to their ~~higher~~high surface smoothness and ~~lower~~low friction to
399 resist water movement. This rapid flow of water can overwhelm natural waterways, increasing the
400 risk of flooding. We used the spatial average of imperviousness across the contributing watershed
401 in ~~the~~our model.

402 ~~Soil category included antecedent soil moisture, which reflects the pre-storm saturation extent,~~
403 ~~essential for runoff estimates and high moisture flux production from rain-bearing systems~~
404 ~~(Ahmadisharaf et al. 2016; Jafarzadegan et al. 2023; Mishra et al. 2022). It is calculated over one~~
405 ~~day before the storm and considered for both "Point specific" and "spatial average across the~~
406 ~~contributing watershed." These values indicate the stream gauge surrounding content and its~~
407 ~~average value over the entire watershed.~~

408 ~~Soil category included antecedent soil moisture, which reflects the pre-storm saturation extent,~~
409 ~~essential for runoff estimates and high moisture flux production from rain-bearing systems~~
410 ~~(Jafarzadegan et al. 2023; Mishra et al. 2022; Karamouz et al. 2022; Ahmadisharaf et al. 2018).~~

411 ~~Soil moisture was calculated one day before the storm and considered both point-based (local soil~~
412 ~~moisture adjacent to the stream gauge) and spatial average across the contributing watershed. This~~
413 ~~feature explains initial conditions in the study watershed.~~

414 In the hydrodynamic category, we used storm surge from tidal gauges on the coast: NOAA
415 (2023). Storm surge was estimated as the difference between the maximum water ~~level~~depth and
416 the astronomical tide during a flood event ~~that was downloaded from NOAA ("NOAA Tides &~~
417 ~~Currents" 2023).~~ This feature is crucial in hindcasting ~~the impact of~~ coastal contributions to flood
418 events. If the flood event does not receive any coastal contributions, this category can be removed

419 from the list of model features. It is considered for both "Point-specific"point-based and "spatial
420 average across the contributing watershed"presenting the stream gauge and its entire watershed
421 tidal condition.

423 2.1.1 Feature selection method

424 We employed commonmultiple feature selection methods,~~such as~~ Pearson's correlation
425 coefficients (Cao et al., 2020; Chen et al., 2023; Lee et al., 2020) and principal component analysis
426 (PCA)~~—~~a widely used technique in many ML modeling studies (Abdrabo et al., 2023; Chang
427 et al., 2022; Reckien, 2018)~~to identify most important features for hindcasting flood depths of a~~
428 given event in a watershed. The PCA components were evaluated based on their absolute values,
429 allowing us to quantify the contribution of each feature to the overall variance. By summing the
430 absolute values across all features, we obtained importance scores for each feature, which enabled
431 us to rank them in descending order. While the Pearson's correlation coefficients are tailored for
432 assessing linear relationships, the PCA captures both linear and non-linear relationships. The
433 strength and direction of linear relationships between the features and flood depth were evaluated
434 using Pearson's correlation coefficient. Through PCA, we determined which principal components
435 in the feature set captured the most variation. These analyses enabled us to narrow down the initial
436 list of the features—and forward feature selection that accounts for interactions among the model
437 features. We applied a step-by-step approach to utilize these three techniques.

438 First, the Pearson's correlation coefficients were used to assessing the linear relationships
439 among the features and target variable. The strength and direction of linear relationships were
440 evaluated using Pearson's correlation coefficients. These analyses enabled us to narrow down the
441 initial list of the features.

442 Next, PCA was applied to the features retained after the Pearson's correlation analysis. In the
443 PCA method, the contribution of each feature to the overall variance is quantified by examining
444 the eigenvalues associated with each principal component (Abdrabo et al. 2023). Compared to the
445 Pearson's linear correlation, the PCA can reveal underlying patterns or structures in the data that
446 are not immediately apparent. PCA allows us to understand how much variance each principal
447 component considers in the dataset, providing a clear measure of feature significance in terms of
448 explaining the data variance. By aggregating the absolute values across all features, we obtained
449 the importance for each feature, which enabled us to rank them in a descending order and omit
450 least important features.

451 Last, the forward selection method was applied on the features retained. This method then
452 incrementally added variables, weighing both their individual impact and interactions, enhancing
453 the model predictive performance by focusing on features with substantial influence on flood
454 depths (Macedo et al. 2019; Horel and Giesecke 2019; Macedo et al. 2019). This method adds
455 variables to a model based on their predictive power. This iterative process starts with no variables
456 and includes the most predictive one at each step, considering both its individual impact and its
457 interactions with already included variables. This selection continues until adding more features
458 does not significantly enhance the model performance metric in terms of Akaike Information
459 Criterion.

461 **2.2. Machine learning (ML) models**

462 2.2.1. Artificial neural networks (ANNs)

463 To hindcast the flood depth, the target variable, we employed ANN. This algorithm was trained
464 via observed flood depths from stream gauges using the key features selected through our feature

465 selection (Section 2.1). The choice of ANN was based on previous successful applications in
466 complex environmental modeling problems (e.g., Adedeji et al., 2022), including flood depth
467 estimations (e.g., Dawson et al., 2006) (Abrahart, Kneale, and See 2004; Bafitihile and Li 2019;
468 Berkahn, Fuchs, and Neuweiler 2019; Dawson et al. 2006; Rumelhart, McClelland, and Group
469 1986; J. J. Zhu, Yang, and Ren 2023). One of the key advantages of using ANN is its capacity for
470 generalization, as highlighted by Maier et al. (2023), allowing the model to perform well on unseen
471 data, making it robust and reliable for real-world flood estimations. Additionally, ANN has been
472 used in flood estimations due to its ability to determine the relationship between rainfall and runoff
473 without relying on specific physical processes, thus addressing the complexities and limitations
474 encountered in hydrologic models (Bafitihile and Li, 2019). ANNs are computing systems inspired
475 by the biological neural networks that constitute animal brains (Dawson et al., 2006, p. 200;
476 McCulloch and Pitts, 1943). They are designed to simulate the behavior of biological systems
477 composed of "neurons". ANNs are composed of nodes, or "artificial neurons", connected and
478 operate in parallel. Each connection is assigned a weight that represents its relative importance.
479 During the learning phase, the network learns by adjusting these weights based on the input data
480 it is processing (McCulloch and Pitts, 1943). ANNs have also been widely utilized in flood
481 estimations due to their ability to model complex relationships and their tolerance for noisy data.
482 Considering the robustness, accuracy, and proven success of ANN in flood estimation tasks, it was
483 deemed suitable for our flood depth estimations. Here, ANN was implemented using python's
484 Keras library with TensorFlow backend.

485

2.2.2. Machine learning (ML) model pre-processing and implementation

The observed flood data and features were split into training and testing sets, with 70% to 90% of the data used for training and 10% to 30% for testing (Joseph 2022; Nguyen et al. 2021). The numerical features in the data were standardized using the StandardScaler function from the Seikit-learn library of python. Hyperparameter optimization is a step in improving the performance of ML models. This process involves identifying the optimal hyper-parameter values for ML classifiers. We used the Random Search cross-validation approach (Boulouard et al. 2022; Hashmi 2020) to perform hyper-parameter optimization. This approach performs a randomized search on hyperparameters using cross-validation. The hyperparameters we optimized here included the number of layers, units, activation functions, optimizer, regularization rate, batch size, and epochs. The best hyperparameters were selected based on the negative mean squared error. The ANN model was trained using the training data and the best hyperparameters obtained from the optimization process. To prevent overfitting, we used early stopping and model checkpointing during the model training. Early stopping was implemented to stop training when the validation loss stopped improving, and model checkpointing was used to save the model with the lowest validation loss. Cross-validation was performed using a 5-fold cross-validation strategy during the hyperparameter optimization process. This strategy involved splitting the training data into five subsets and training the model five times, each time using a different subset as the validation set. We allocated 90% of the data for training and 10% for testing. While the portion for test is small, the utilization of cross-validation, randomized hyperparameter search, early stopping, and model checkpointing collectively works to construct a model less susceptible to overfitting on a particular test set. This allocation of 10% for testing, combined with these methodologies, is designed to enhance the model's ability to generalize across diverse scenarios.

509
510 To hindcast flood depth, our target variable, we employed ANN with MLP architecture. This
511 algorithm was trained via observed maximum water depths from stream gauges using the key
512 features selected through our feature selection (Section 2.1). The choice of ANN was based on
513 previous successful applications in flood depth modeling (e.g., Dawson et al., 2006; Abrahart,
514 Kneale, and See 2004; Bafitlhile and Li 2019; Berkhahn, Fuchs, and Neuweiler 2019; Dawson et
515 al. 2006; Rumelhart, McClelland, and Group 1986; Zhu, Yang, and Ren 2023). One of the
516 strengths of using ANNs in modeling tasks like flood predictions is their notable flexibility and
517 capability to approximate complex, non-linear relationships, potentially enhancing their
518 performance for unseen data. It is essential, however, to acknowledge that the capacity to
519 generalize depends on selecting relevant features that explain the underlying physical processes
520 and the spatiotemporal variability, model selection, parameterization, and training the model.
521 ANNs are designed to simulate the behavior of biological systems composed of "neurons". These
522 algorithms composed of nodes, or "artificial neurons", connected and operate in parallel. Each
523 connection is assigned a weight that represents its relative importance. During the learning phase,
524 the network learns by adjusting these weights based on the input data it is processing (McCulloch
525 and Pitts, 1943). Here, ANN was implemented using python's Keras library with TensorFlow
526 backend.

527
528 2.2.2. Machine learning (ML) model pre-processing and implementation

529 The observed water depths and features were split into training and testing sets, with 70% to
530 90% of the data used for training and 10% to 30% for testing as suggested by Joseph (2022) and
531 Nguyen et al. (2021). After exploring various splits within the 70% to 90% range for training data,

532 the 90% allocation for training (104 out of 116 stream gauges) was determined to be optimal for
533 our specific dataset and model based on preliminary testing, the model complexity, and the desire
534 to maximize the amount of data used for training while still retaining satisfactory results for the
535 test phase (12 out of 116 stream gauges). While the train percent (90%) seems high and suggests
536 potential for model overfitting, this same model was most successful in the transferability across
537 other three flood events (out-of-sample). The allocation of 10% of the data for testing serves to
538 provide an unbiased appraisal of the model generalization performance after training and
539 hyperparameter optimization. This evaluation process, complemented by methodologies such as
540 cross-validation and hyperparameter optimization, is structured to identify a model configuration
541 that is likely to perform well across unseen data. This approach aims to ensure that the final model,
542 selected based on its performance on the validation set during hyperparameter optimization, is
543 tested on entirely unseen data to confirm its generalization ability. In preparing our dataset for the
544 neural network model, numerical features were standardized to have a mean value of zero and a
545 standard deviation of one. This scaling process ensured that each feature contributes
546 proportionately to the model predictions, mitigating the potential bias towards variables with larger
547 scales.

548 Hyperparameter optimization is a step in improving the performance of ML models. This
549 process involves identifying the optimal hyper-parameter values. We used Bayesian Search to
550 perform hyperparameter optimization. Cross-validation, particularly through methodologies like
551 the Prediction Sum of Squares criterion for predictor selection and for parameter estimation and
552 predictive error assessment, has been foundational in improving predictive models. This approach
553 distinguishes between model selection and assessment (Allen 1974; Geisser 1975; Stone 1974).
554 Cross-validation was performed using a 5-fold cross-validation strategy during the hyperparameter

555 optimization process. Opting for 5-fold cross-validation over hold-out validation in our
556 hyperparameter optimization process reflects a balance between comprehensive model evaluation
557 and computational efficiency. The hyperparameters we optimized here included the number of
558 layers, units, activation functions, optimizer, regularization rate, batch size, and epochs. Bayesian
559 search offered a targeted search based on probabilistic modeling, iteratively refining the search
560 area based on past evaluations to efficiently select the most promising hyperparameter sets. The
561 selection of the optimal hyperparameters was guided by minimizing the cross-validation MSE,
562 ensuring the chosen configuration significantly improved the model predictive performance for
563 maximum water depths. The ANN-MLP model was trained using the training data and the best
564 hyperparameters obtained from the optimization process.

565 To prevent overfitting, we used early stopping and model checkpointing during the model
566 training. Early stopping was implemented to stop training when the validation loss stopped
567 improving, and model checkpointing was used to save the model with the lowest validation loss.
568 The strategy involved splitting the training data into five subsets and training the model five times,
569 each time using a different subset as the validation set. This evaluation process, complemented by
570 methodologies such as cross-validation and hyperparameter optimization, is structured to identify
571 a model configuration that is most likely to perform well across unseen data.

572 2.2.3. Model performance evaluation

573 The performance of the ANN-MLP model was evaluated using coefficient of determination (R^2),
574 ~~Mean Absolute Error~~ mean absolute error (MAE), ~~Normalized Root Mean Square Error~~ normalized
575 root mean square error (NRMSE), median absolute error (MDAE), and the ratio of estimated over
576 the observed maximum flood depth (F_Q ; Schubert and Sanders 2012). The R^2 metric measures the
577 proportion of variance in the dependent variable predictable from the independent variables. The

Formatted: Indent: First line: 0"

Formatted: Superscript

578 MAE measures the average magnitude of the errors in a set of estimations without considering
579 their direction (i.e., overestimation or underestimation). The NRMSE is a metric that quantifies
580 the normalized average magnitude of the prediction error. It assesses the relative size of the root
581 mean square error (RMSE) by considering the RMSE in relation to the average value of the
582 ~~observation~~observations. It is commonly used in regression ~~analysis~~analyses and a smaller
583 NRMSE value indicates a higher level of agreement between the estimated values and the actual
584 observations (Stow et al. 2003; Ahmadisharaf Ebrahim et al. 2019). ~~These metrics were calculated~~
585 ~~for both training and testing datasets to assess the model performance.~~The MDAE is a metric that
586 measures the median of the absolute differences between predicted values and actual (observed)
587 values. Unlike the MAE, which averages these differences out, the MDAE focuses on the midpoint
588 of these differences, making it less sensitive to the outliers. This characteristic can make the
589 median error a more robust metric in the regional water depth estimation where the data contains
590 significant outliers. It is a common metric used in ML models such as Sheridan et al. (2019); Dixit
591 et al. (2022); Park, Ju, and Kim (2020). These metrics were calculated for both training and testing
592 datasets to assess the model performance.

593

594 2.2.4. Model ~~interpretation~~explainability

595 To interpret the model and ~~understand~~explore the contribution of each feature to the estimation,
596 we used ~~SHapley Additive exPlanations~~ (SHAP) that is a game theoretic approach to explain the
597 output of an ML model (Lundberg and Lee, 2017). It connects optimal credit allocation with local
598 explanations using the classic Shapley values from game theory and their related extensions. The
599 SHAP values interpret the impact of having a certain value for a given feature in comparison with
600 the estimations we would make if that feature took some baseline value (Abdollahi and Pradhan,

601 2021). In other words, SHAP estimates how much each feature contributes to the ~~predictive~~-model
602 prediction output for a particular instance. The SHAP results on the feature importance and their
603 impacts on the model ~~estimation~~prediction can be presented using a plot to visually show the
604 distribution of impacts of each feature on the model output. A positive SHAP value indicates that
605 the feature's presence increases the model output, while a negative SHAP value indicates that it
606 decreases the model output. Further, we visually evaluated the performance of our model in terms
607 of bias (overestimation and underestimation) using scatter plots.

Formatted: Indent: First line: 0"

609 2.3. Model transferability across flood events

610 The ML-based model, which was initially developed, trained, and validated based on one flood
611 event, was subsequently examined as is (with no additional parameter tuning) against other events
612 in terms of the performance and generalizability in hindcasting maximum floodwater depths. By
613 examining our model against different flood events, we aimed to evaluate its effectiveness in
614 hindcasting floodmaximum water depths across diverse events. This evaluation allowed us to
615 assess the ML ~~model's~~model ability to handle varying flood conditions and its potential for
616 application in different events in the same watershed.

Formatted: Indent: First line: 0.25"

618 3. Study area

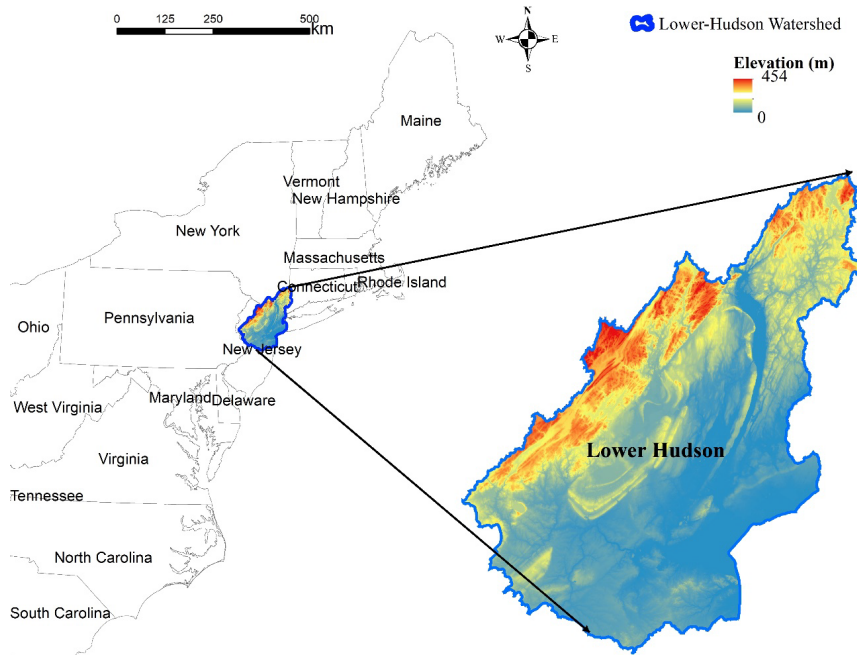
619 The study area is a HUC6 watershed, the Lower Hudson Watershed ~~a six-digit hydrologic unit~~
620 ~~code (HUC 020301) according to the USGS classification.~~ The 10,068 km² watershed is in the
621 Northeastern United States (Figure 2) spanning parts of three states, Connecticut, New Jersey, and
622 New York. This watershed has a humid subtropical climate with hot summers and mild winters.
623 The highest elevation is ~450 m above mean sea level. Residential, agriculture, and forest are the

624 dominant land uses in the watershed according to the ~~2022~~2021 National Land Cover Dataset
625 (NLCD) (USGS 2022). Large metropolitan areas like New York are in the study watershed. ~~The~~
626 ~~population density was estimated at 344 persons per square km in 2020 (USCB, 2020), with higher~~
627 ~~concentrations in urban areas like New York and lower densities in rural parts.~~ Several major rivers
628 drain into the watershed, including the Hudson River, which flows for 496 km (about the length
629 of New York State). The ground slope varies from 87.5% in the mountainous parts to ~~0%~~near zero
630 in the coastal ~~region~~parts.

631 We studied four major flood events in the study area. The primary event for model
632 development was Hurricane Ida in 2021, while three other hurricanes—Isaias (2020), Sandy
633 (2012) and Irene (2011)—were used to assess the model transferability. Hurricane Ida, a
634 devastating Atlantic Category 4 hurricane that made landfall in September 2021, hit Louisiana,
635 and progressed toward the Northeastern United States. The hurricane caused considerable floods
636 and significantly impacted both the west-south-central region, including New Orleans, and the
637 northeastern region, with severe damages reported in New York City and Philadelphia (~~Beven II,~~
638 ~~Hagen, and Berg 2022; J. Wang et al. 2022~~)(~~Beven II, Hagen, and Berg 2022; Wang et al. 2022~~).

639 The storm remnants sent record-breaking rainfall to the New York region as they headed northeast,
640 resulting in flash flooding (Beven II, Hagen, and Berg 2022). The extensive flooding and severe
641 property destruction caused by Hurricane Ida's record-breaking rains highlighted the importance
642 of comprehending the hurricane effects on affected areas. Furthermore, strengthening regional
643 resilience to catastrophic flooding episodes requires the development of effective mitigation
644 strategies. The three other events, which were used to evaluate the model transferability, were also
645 most recent major hurricanes after 2000, with available ~~stream gauge~~streamflow data and differing
646 track and intensity. In 2020, Hurricane Isaias, a Category 1 hurricane, made a quick trip along the

647 East Coast, bringing with it severe rain and floods, especially in the Mid-Atlantic and Northeast.
648 The storm's rapid passage caused several deaths and extensive power losses (Latto, Hagen, and
649 Berg 2021). In 2012, superstorm Sandy, commonly known as Hurricane Sandy, struck the
650 Northeast and caused severe damage. It produced significant flooding due to the intense storm
651 surge and torrential rains, especially in New York and New Jersey, where the storm surge reached
652 record heights (Blake et al. 2013). In 2011, a huge and catastrophic storm named Hurricane Irene
653 affected a major portion of the Eastern Seaboard. Heavy rains from the storm caused significant
654 flooding, especially in Vermont, where it was the worst flooding in over a century for that state
655 (Lixion ~~A~~ and Cangialosi 2013).



656
657 Figure 2.2. Lower Hudson River Watershed.

Field Code Changed

Formatted: Keep with next

Formatted: Caption, Left

658

659 3.1. Data collection

660 Table 2 lists the data used for the study area alongside their source and ~~spatial and~~
 661 ~~temporal~~ spatiotemporal resolutions. We acquired instantaneous stream gauge height data from the
 662 USGS’s National Water Information System to analyze water ~~levels~~ depths during the four flood
 663 events. While the features’ data had different spatial resolutions, we did not make them consistent
 664 because only at-point (stream gauges) or aggregated spatial statistics of contributing watersheds
 665 were used in the ML model; no combinations of the features were needed.

666 Table 2. Model features and data sources and resolutions in the study area. NHDPlus: National
 667 Hydrography Dataset Plus; NED: National Elevation Dataset; NWIS: National Water
 668 Information System.

Formatted: Caption, Left, Indent: First line: 0", Keep with next

<u>Category</u>	<u>Feature</u>	<u>Source</u>	<u>Spatial resolution</u>	<u>Temporal resolution</u>
<u>Geographic location</u>	<u>Distance to rivers</u>		==	==
	<u>Distance from storm track</u>	<u>NHDPlus</u>	==	==
	<u>Distance from the coastline</u>		==	==
<u>Hydrologic</u>	<u>Height above nearest drainage (HAND)</u>	<u>NED</u>	<u>10 m</u>	==
	<u>Drainage area</u>	-	==	==
	<u>Flow accumulation</u>	-	==	==
	<u>Topographic wetness index (TWI)</u>	-	==	==
<u>Meteorologic</u>	<u>Initial water depth</u>	<u>NWIS</u>	-	-
	<u>Rainfall depth</u>			
	<u>Wind speed</u>	<u>NCEI</u>	==	<u>Daily</u>
<u>Topographic</u>	<u>Elevation</u>			==
	<u>Ground slope</u>			==
	<u>Invariability of slope directions (ASPVAR)</u>	<u>NLCD</u>	<u>10 m</u>	==
<u>Land surface</u>	<u>Curvature</u>			==
	<u>Imperviousness</u>	<u>NLCD</u>	<u>30 m</u>	==
<u>Soil</u>	<u>Antecedent soil moisture</u>	<u>ERA5</u>	==	<u>Daily</u>
<u>Hydrodynamic</u>	<u>Storm surge</u>	<u>NOAA Tides and Currents</u>	==	<u>Sub-hourly</u>

Formatted: Font: (Default) +Headings CS (Times New Roman)

Formatted: Indent: First line: 0.25"

669

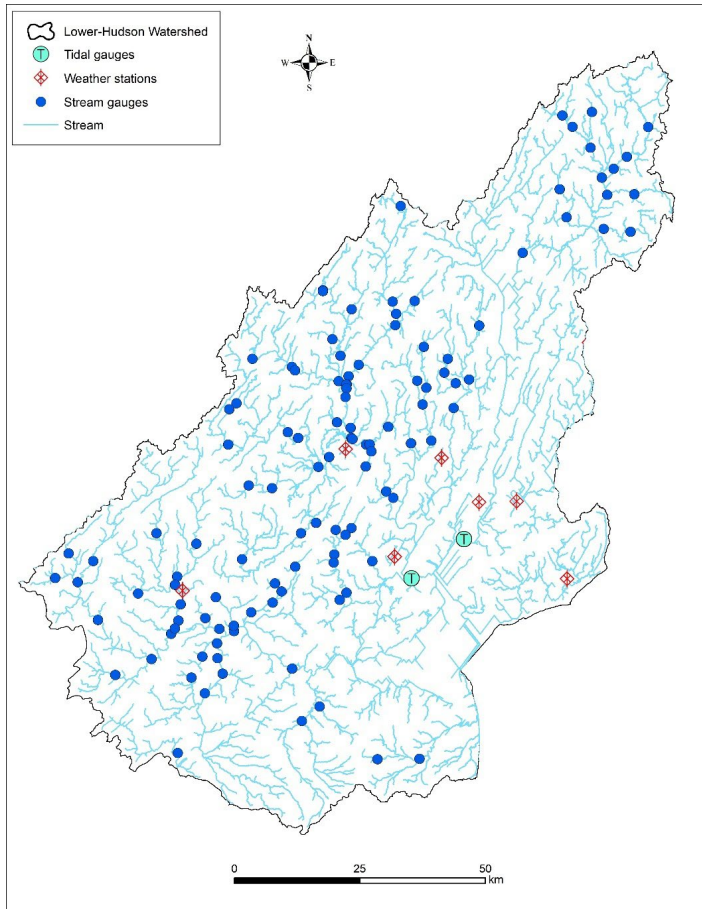
670 The study watershed embraces 116 stream gauges, seven weather stations and two tidal gauges
671 (Figure 3). These gauges and stations recorded ~~the~~ data for all the four events (Hurricanes Ida,
672 Isaias, Sandy, and Irene). The drainage area of the contributing watersheds of the stream gauges
673 varies from 5.5 to 2,104 km². The range of maximum recorded ~~flood-maximum water~~ depths,
674 rainfall, and antecedent soil moisture ~~at~~near the stream gauges during the four hurricanes are
675 presented in Table 23. It shows that ~~Hurricane Ida had a narrower range of water levels, even~~
676 ~~though it generated lower cumulative-~~Hurricanes Ida and Irene associated with much higher
677 rainfall depths. ~~In contrast, Hurricane Irene had the broadest range in river water levels, likely~~
678 ~~due~~These increased precipitation levels contribute directly to the significant amount of rainfall it
679 ~~encountered during the event. Also,~~flood severity, as they can overwhelm drainage systems and
680 lead to runoff exceeding riverbank capacities. The percent soil moisture before the storms ranged
681 from fairly dry conditions (9%) to nearly half saturated (43%). Ida and Irene had similar antecedent
682 soil moisture conditions, which ~~could have~~ influenced their respective river water ~~levels~~depths.
683 Hurricane Sandy had a higher antecedent soil moisture percentage range of 17% to 38% compared
684 to both Ida and Isaias, indicating a potentially higher level of saturation before the ~~storm's~~storm
685 arrival. This ~~may have~~likely contributed to Sandy's significant storm surge, which ranged from
686 1.97 to 2.85 m, compared to Ida and Isaias with storm surge ranges of 0.25 to 0.67 m and 0.20 to
687 0.76 m, respectively. Maximum wind speeds during these events were quite high, especially for
688 Hurricanes Isaias, Sandy, and Irene. The proximity to the central path of the storm influences the
689 intensity of the rainfall, wind speed, and storm surge experienced. Shorter distances to the storm
690 track, particularly in Ida and Irene, correlated with more severe weather conditions and,
691 consequently, greater flood depths.

693 Table 23. The range of river water leveldepth, cumulative rainfall depth and antecedent soil
 694 moisture in the flood events.

Formatted: Caption, Left, Keep with next

<u>Hurri eaneE vent</u>	Year	River water <u>leveldepth</u> (m)	Cumulative rainfall depth (mm)	Antecedent soil moisture (%)	Storm Surge (m)	Wind <u>Max</u> <u>speed</u> (m/s)	Distance to storm track (m)
Ida	2021	0.85-36.66	0.01- 45.43 121.92- 201.81	21-43%	0.25-0.67	27.64-35.49	0.09-1.1
Isaias	2020	0.22-35.35	17.37-62.22	9-39%	0.20-0.76	48.29-65.33	0.23-1.14
Sandy	2012	0.24-35.98	19.83-56.53	17-38%	1.97-2.85	63.43-76.97	0.77-2.16
Irene	2011	1.03-37.33	147.29-217.74	19-43%	1.05-1.37	51.05-60.68	0.00-0.93

Formatted: Left, Indent: First line: 0"



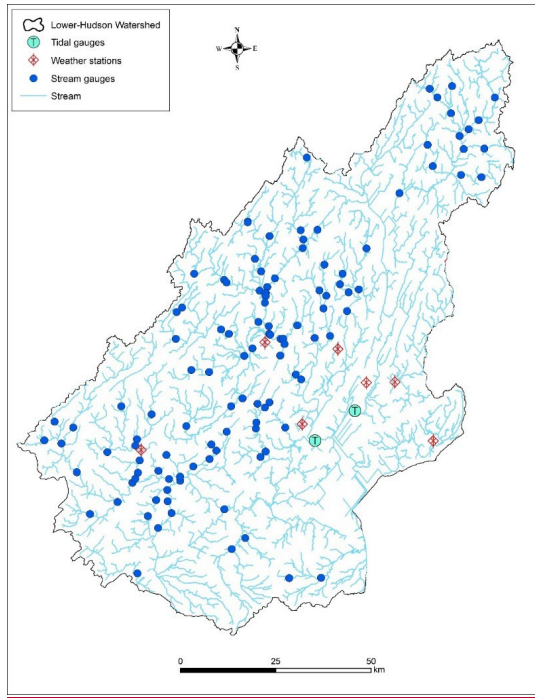


Figure 3-3. Stream and tidal gauges and weather stations in the study watershed.

Formatted: Caption, Left, Indent: First line: 0"

~~Table 3: Model features and data sources and resolutions in the study area. NHDPlus – National Hydrography Dataset Plus; NED – National Elevation Dataset; USGS NWIS – United States Geological Survey National Water Information System; NCEI – National Centers for Environmental Information; NLCD – National Land Cover Database; ERA5 – Fifth Generation of the European Centre for Medium Range Weather Forecasts (ECMWF) Reanalysis; NOAA – National Oceanic and Atmospheric Administration.~~

Formatted: Caption, Left, Indent: First line: 0", Keep with next

Category	Feature	Source	Spatial resolution	Temporal
----------	---------	--------	--------------------	----------

				resolution #
Geographic location	Distance to rivers		—	—
	Distance from storm track	NHDPlus	—	—
	Distance from the coastline		—	—
Hydrologic	Height above nearest drainage (HAND)	NED	10-m	—
	Drainage area	-	—	—
	Flow accumulation	-	—	—
	Topographic wetness index (TWI)	-	—	—
Meteorologic	Rainfall depth			
	Wind speed	NCEI	—	Daily
Topographic	Elevation			—
	Ground slope	NLCD	10-m	—
	Slope aspect invariability (ASPVAR)			—
	Curvature			—
Land surface	Imperviousness	NLCD	30-m	—
Soil	Antecedent soil moisture	ERA5	—	Daily
Hydrodynamic	Storm surge	NOAA Tides and Currents	—	Sub-hourly

706

707

708

709

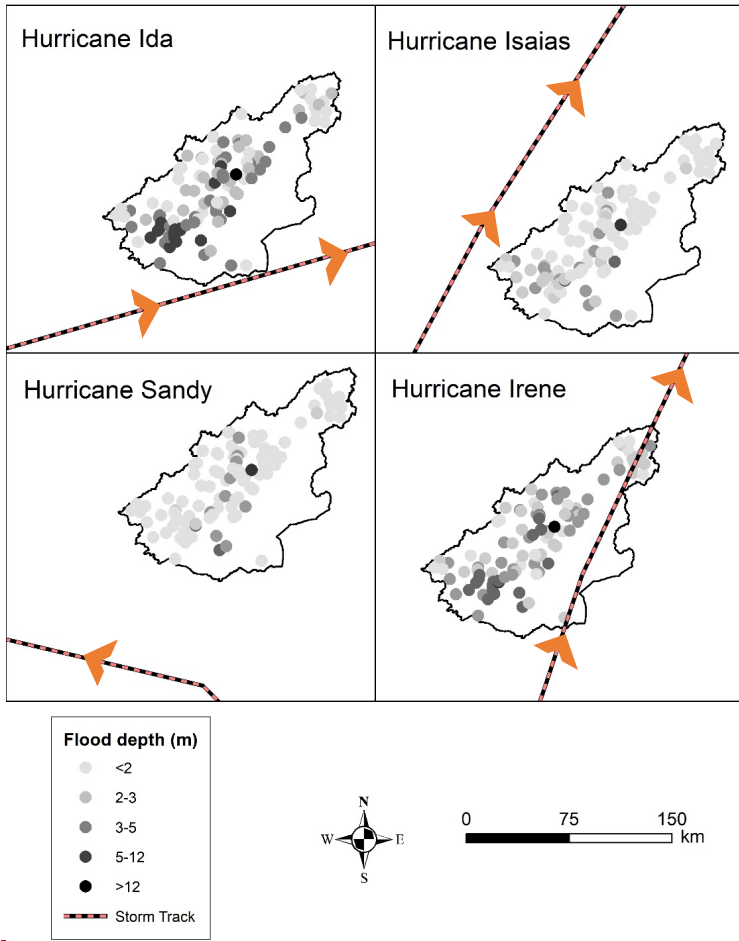
710

Figure 4 displays the ~~variations in~~spatial variability in maximum water levelsdepths and storm tracks for all hurricanes. The total slope aspect ~~is~~was south, which ~~results~~resulted in shallower depths at the ~~upper point of the river~~upstream. As we ~~move~~moved southward along the ~~river's~~river mainstream, ~~water depths became~~ deeper ~~water levels are observed~~.

Formatted: Font: (Default) +Headings CS (Times New Roman)

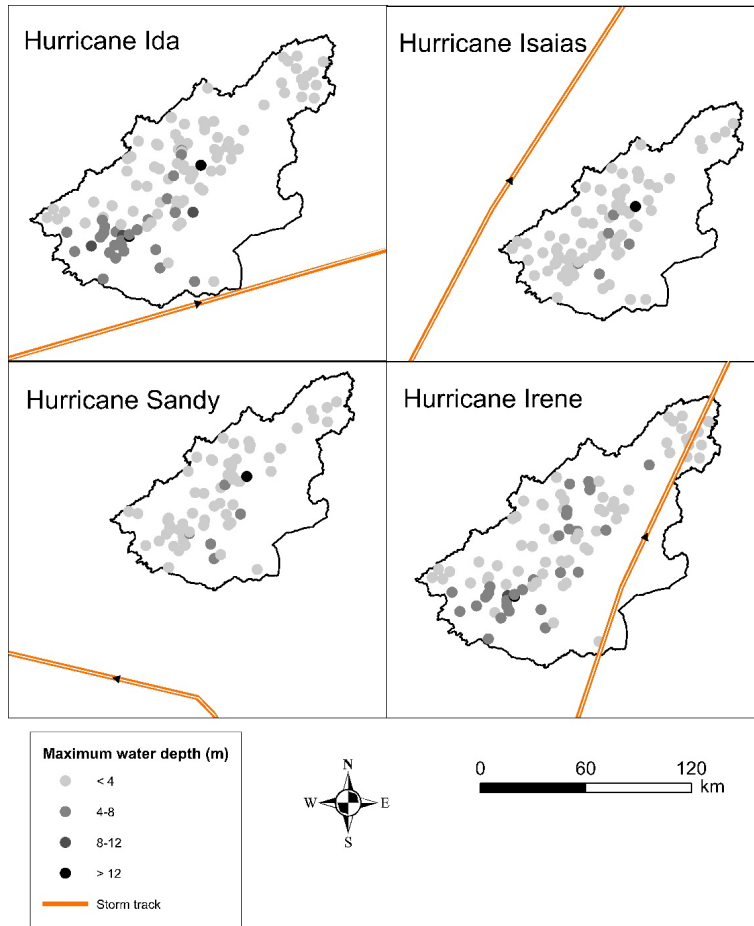
Formatted: Indent: First line: 0.25"

Formatted: Justify Low



712

Figure 4. Water levels



713

714 Figure 4. Maximum water depths across the study area during ~~studied~~ the four study hurricanes.

Formatted: Centered, Indent: First line: 0", Keep with next

715

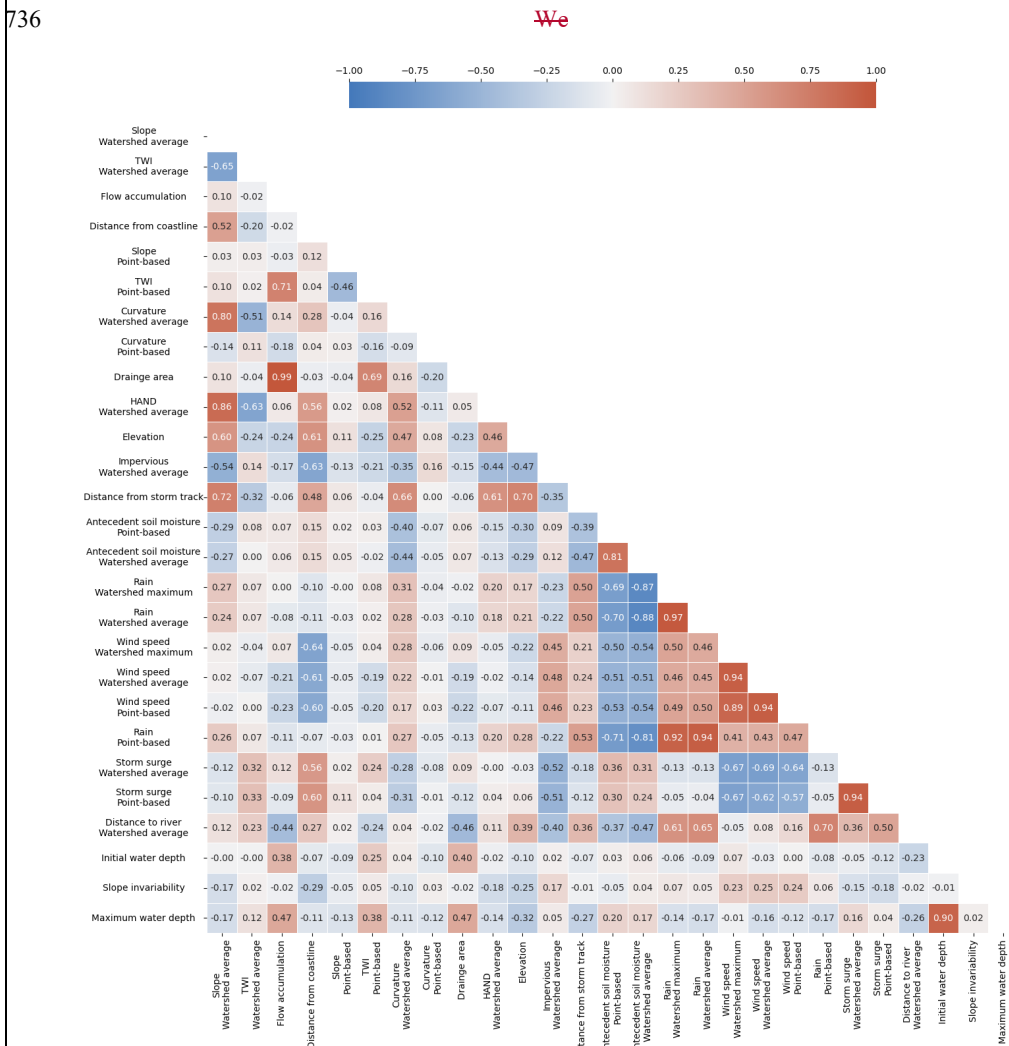
716 **4. Results and discussion**

717 **4.1. Feature selection**

718 4.1.1. Pearson's correlation matrix

719 ~~As a result of Using~~ Pearson's correlation analyses, we eliminated five features with absolute
720 correlation coefficients ~~greater than~~ ≥ 0.70 , the cutoff threshold suggested in previous studies (Cao
721 et al. 2020; Chen et al. 2023; Lee et al. 2020). ~~The~~ According to Figure 5, the strong correlation
722 coefficient of 0.99 between "Drainage drainage area" and "Flow flow accumulation", indicated that
723 both variables/features capture similar information about water flow and storage in the watershed.
724 To avoid collinearity issues, "Flow flow accumulation" was excluded from further analyses.
725 ~~Similarly, the high due to its weaker~~ correlation ~~coefficient of 0.97 between "Rain-MAX" and~~
726 ~~"Rain-Mean" suggested with flood depth. Similarly, features that they offer similar information~~
727 ~~about maximum and average rainfall values across the watershed. Consequently, "Rain-Mean"~~
728 ~~was demonstrated weaker correlations with flood depth or were highly correlated with multiple~~
729 ~~features, were excluded from consideration. Additionally, a correlation coefficient of 0.94 between~~
730 ~~"Tide Mean" and "Tide Point" indicated that the average tide level within the watershed closely~~
731 ~~resembled tide levels measured at stream gauge points. As a result, "Tide Point" was excluded~~
732 ~~from the analysis. By considering the correlation coefficients and the potential redundancy among~~
733 ~~features, we. These analyses~~ ensured that independent variables, which are essential for modeling
734 flood maximum water depths, are ~~selected~~ retained in our modeling.

735 4.1.2. Principal Component Analysis (PCA)



737

738 Figure 5. Heatmap of Pearson correlation matrix for the initial model features.

739 ~~Next, we~~ conducted PCA to assess the importance of ~~various~~the features ~~retained by Pearson's~~
740 ~~correlation analyses~~ in hindcasting ~~flood~~maximum water depths. The ~~results of the PCA analysis~~
741 ~~unveiled the key features~~analyses showed that ~~significantly influence~~ the ~~flood depth~~.

742 Interestingly, we identified the "Slope Point", river slope at the stream gauges, "Slope
743 Aspect",gauge, slope aspect, slope invariability, curvature at the stream gauge, and distance from
744 average curvature across the coastline as contributing watershed were the least key important
745 features for capturing the overall variability of maximum flood depth. Consequently, we excluded
746 ~~these features~~ from ~~further~~our analyses. The lesser importance of "Slope Point"slope at the
747 stream gauge and "Slope Aspect"slope aspect may be since river slope is related to bathymetry,
748 which is typically not represented well by DEMs (Bhuyian and Kalyanapu 2020).

749 The forward feature selection method showed that initial water depth, elevation, TWI,
750 antecedent soil moisture, rainfall, and distance from storm surge at the stream gauge (all point-
751 based), as well as average storm surge and maximum wind speed across the contributing
752 watershed, along with their interactions were selected for the final ML model. Considering the
753 interactions among the features improved the model performance. This was expected because a
754 combination of some of the features better explain the underlying physical processes. For instance,
755 using the combination of storm surge and TWI as one unified feature can be an indication of the
756 physical propagation of storm surge that occur primarily in waterways.

758 4.2. Machine learning (ML) model development

759 4.2.1. Model development and performance evaluation

760 ~~We conducted a thorough hyperparameter optimization process to fine-tune the neural network~~
761 ~~model for estimating the flood depth of Hurricane Ida. The optimization process involved 500 fits,~~

Formatted: Indent: First line: 0.25"

Formatted: Font: (Default) +Headings CS (Times New Roman), 12 pt, Font color: Auto

Formatted: Left, Indent: First line: 0"

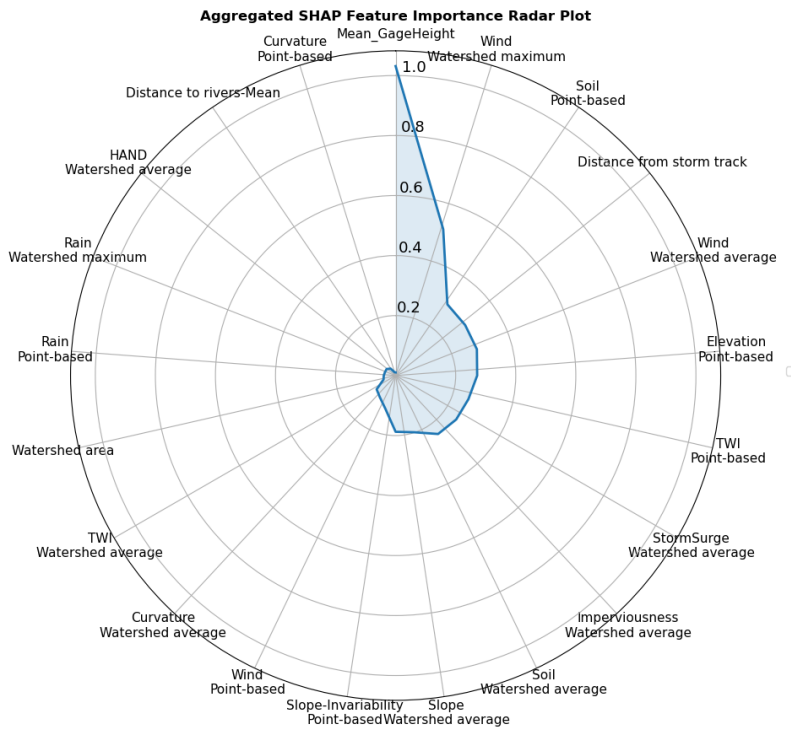
762 with each fit considering 100 candidates for each of the five folds in the cross-validation. This
763 helps to ensure that the model's performance is robust and not dependent on a specific
764 training/testing split. As a result, the model became more effective in making estimations on
765 unseen data, as indicated by the enhanced testing performance. Furthermore, the optimization
766 process allowed us to find the best combination of hyperparameters that optimized the model's
767 performance. The best hyperparameters were identified as follows: 50 units, a regularization rate
768 of approximately 0.104, the *sgd* optimizer, one layer, 600 epochs, a batch size of 8, and the *elu*
769 activation function. These optimized hyperparameters were then used to train the ANN model and
770 evaluate its performance. This meticulous hyperparameter optimization approach ensured that the
771 model was fine-tuned to achieve the best possible performance for estimating flood depths.

772 In the development of our ANN-MLP model for hindcasting maximum water depths during
773 Hurricane Ida, we used Bayesian search with a cross-validation strategy for hyperparameter
774 optimization. Details of the optimization can be found in Supplementary Material.

775 The model demonstrated an excellent performance on the training dataset, with an (R^2 of 0.93,
776 indicating that the model can explain 93% of the variance in the training data. The 0.94, MAE
777 for the training data was 0.64 m, MDAE = 0.44 m, and NRMSE was 28%, suggesting that the
778 model estimations were satisfactory. 24%). On the test dataset, the model achieved an R^2 of
779 0.87, the MAE of 0.8777 m, MDAE was 0.42 m, and the NRMSE was 33%. These values also
780 show that 28%, further suggesting the model's performance was satisfactory during performance by
781 the test phase but slightly poorer than the train phase model. The training history plot showed that
782 the model performance improved with each epoch during training, indicating that the model was
783 learning from the data. The model training process stopped at epoch 7587 due to early stopping.

785 4.2.2. Model interpretation/explainability

786 ~~Figure 5 provides an overview of the influence of distinctive features on the model estimation~~
787 ~~on flood depths. The SHAP values measure the contribution of a feature to the estimation for each~~
788 ~~sample in comparison to the estimation made by a model trained without that feature.~~

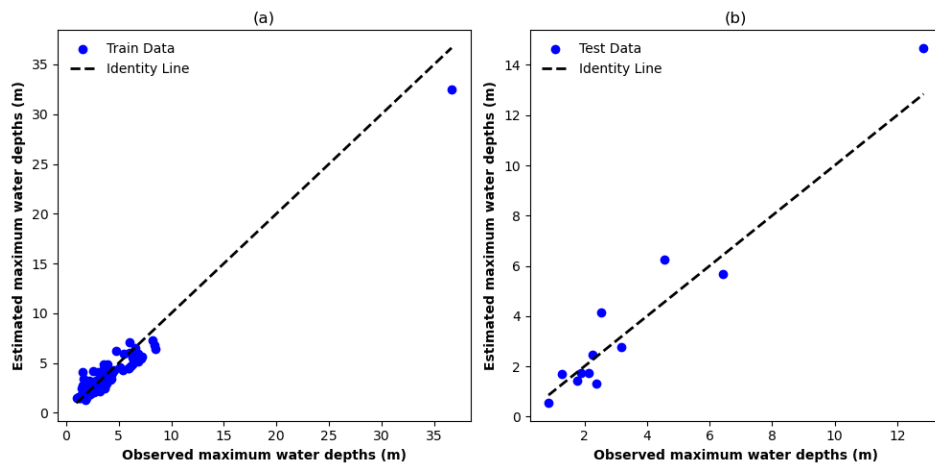


789 ~~Figure 5. Shapely additive explanations (SHAP) summary plot of the flood model.~~

790 ~~The most influential features in estimating flood depths are antecedent water level, indicating that~~
791 ~~streams with higher water levels before an event are subject to greater flood depths. When~~
792 ~~combined with additional rainfall or water input during a flood, they lead to increased flood depths.~~

795 Similarly, spatial maximum wind speed across the contributing watershed, antecedent soil
796 moisture at point, and elevation are other significant factors affecting flood depth estimations, with
797 greater values associated with higher estimated flood depths. Intense winds during a hurricane
798 accelerate the movement of floodwaters, leading to greater depths in certain areas, while saturated
799 soil has limited capacity to absorb additional water, resulting in more surface runoff and higher
800 flood depths. Figure 6 shows the performance of the ML model in hindcasting maximum water
801 depths at stream gauges, comparing estimated values against observed values for both training and
802 testing datasets. In the training phase (Figure 6a), points are clustered along the identity line, but
803 tend to underestimate large water depths. This pattern suggested that the model learned the training
804 data well, especially for smaller water depths, but did not fully capture the behavior that leads to
805 the larger water depths. The underestimation of high values is expected due to the lower number

806 of observations. The test data (Figure 6b) revealed a similar pattern of underestimation towards
807 higher values; this can be since the number of observed high water depths is small.



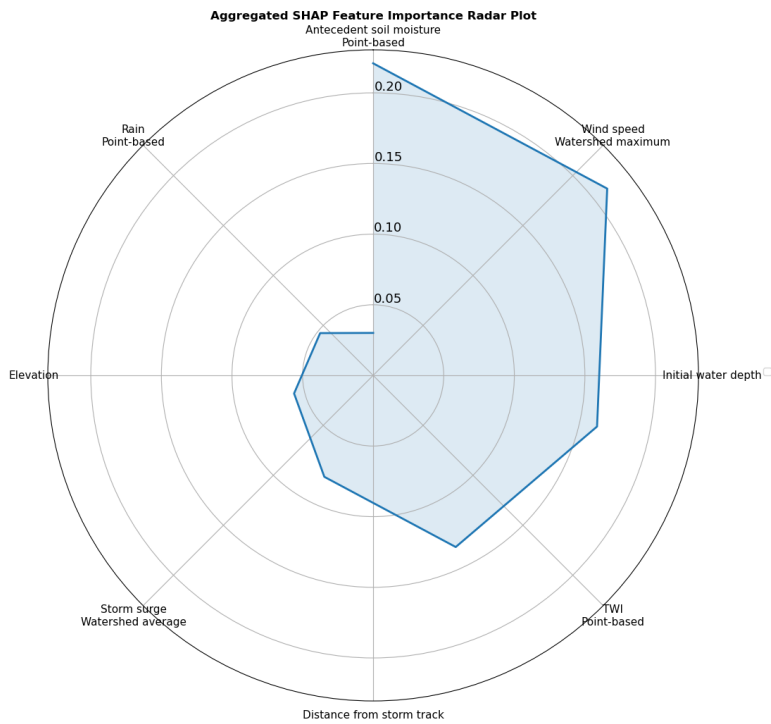
808
809 Figure 6. Scatter plots of estimated vs observed maximum water depths for: (a) train and (b) test
810 data. The identity line represents a perfect match between the estimated and observed values.

811 Figure 7 provides an overview of the influence of distinctive features on the model estimation
812 on maximum water depths. Features like the antecedent soil moisture and maximum wind speed
813 across the contributing watershed were found to substantially influence the water depth
814 estimations. The inclusion of elevation as an important feature in our study closely aligns with the
815 findings of Hosseini et al. (2020) and Chen et al. (2023) in their flash flood susceptibility and
816 hazard ~~assessment-one~~assessments on a small non-coastal watershed ~~tidal~~ and ~~the other on~~ a large
817 coastal watershed. Elevation has been ~~consistently~~ recognized as a crucial factor influencing flood
818 occurrences, as it directly affects the water flow and drainage patterns within a watershed (Rafiei-
819 Sardooi et al. 2021).

820 On the other hand, features such as the spatial average of distance to rivers across the
821 contributing watershed, the spatial average of HAND across the contributing watershed, and
822 rainfall both at point and the spatial maximum of it across the watershed were identified as the
823 least key features in estimating flood depths. This can be attributed to the fact that our target is
824 hindcasting flood depths at stream gauges, while these input features are more associated with
825 flood depths occurring away from the stream network. Consequently, these features exhibit a
826 limited impact on the model predictive performance when compared to other factors. The spatial
827 average of distance to rivers and HAND have limited variability within our watershed and might
828 not fully capture relevant information about geography, topography, and drainage patterns, leading
829 to reduced discriminatory importance in flood depth estimation models.

830 The finding about the less importance of rainfall in flood estimation concurs with the results
831 reported in the study by Salvati et al. (2023) in pinpointing vulnerable regions within a non-coastal
832 medium-sized watershed. The study suggests that rainfall may have a lower impact on flood
833 occurrences or flood depth estimations compared to other influential factors. This highlights the
834 significance of considering a comprehensive set of variables in flood modeling to accurately
835 capture the underlying relationships and improve estimation performance. The model ability to
836 capture these complex relationships demonstrated its potential utility in flood estimation and
837 management.

838



839 Figure 7. Aggregated Shapely additive explanations (SHAP) feature importance radar plot of the
 840 ML model for hindcasting maximum water depths.
 841

842 On the other hand, features such as the interaction of initial water depth and rainfall and local
 843 rainfall were identified as the least key features in estimating maximum water depths. In a coastal
 844 context, where the landscape reaction to oceanic events often overshadows rainfall affect, this
 845 outcome is noticeable. The finding about the less importance of rainfall in flood estimation concurs
 846 with the results by Salvati et al. (2023) in pinpointing vulnerable regions within a non-coastal
 847 medium-sized watershed. The study suggested that rainfall may have a lower impact on flood
 848 occurrences or flood depth estimations compared to other influential factors. The consideration of

the interactions between rainfall and other features may also obscure the direct influence of rainfall on the model's predictions, especially in complex flood modeling.

It is important to note that the least important features are not necessarily uninformative; they simply contribute less to the model's output relative to the most important features. This can be due to the nature of the data, the modeling approach, or the specific context of the problem being addressed.

4.3. Examining the machine learning (ML) model transferability across flood events

The transferability of the trained and tested model (against Hurricane Ida) was examined by applying it to three other events within the same watershed. Table 4 summarizes the evaluation metrics for the three hurricanes.

Table 4. Model performance across in historical flood events. MAE—; mean absolute error; MDAE: Median Absolute Error; RMSE—; root mean square error; F_Q —; ratio of estimated over observed maximum flood depth.

Flood event	R ²	MAE (meters)	MDAE (%)(meters)	NRMSE (%)	F _Q (%)
Original Model					
Hurricane Ida	0.9294	0.6664	290.45	24.1	138.1
Transferability					
Hurricane Isaias	0.7773	1.4454	800.85	32286.3	325.6
Hurricane Sandy	0.70	1.71	1.6978	109.2	366370.2
Hurricane Irene	0.885	1.4912	430.85	11336.7	112.6

These results demonstrated the model ability to generalize/transfer across different hurricanes within the same watershed ($R^2 > 0.7$). With an MAE less than 1.6971 m in all hurricanes, our

Formatted: Left, Indent: First line: 0"

Formatted: Caption, Left, Keep with next

Inserted Cells

Inserted Cells

Formatted Table

Inserted Cells

Inserted Cells

Inserted Cells

Inserted Cells

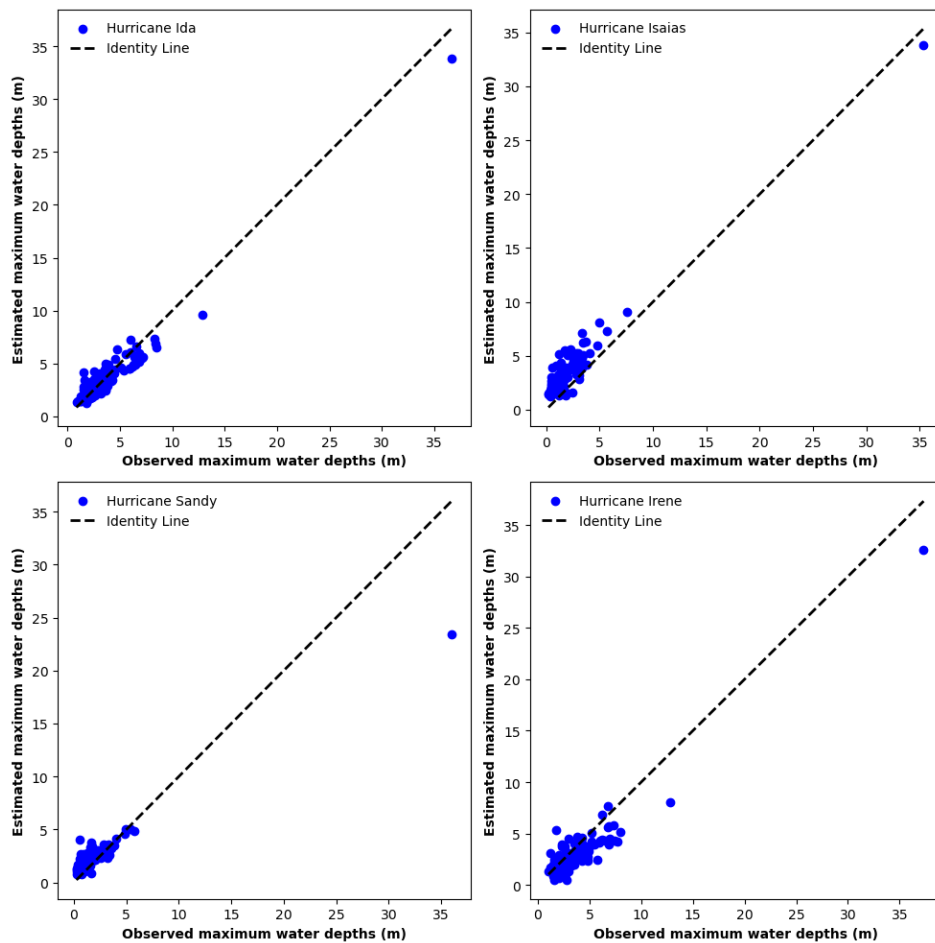
Formatted: Indent: First line: 0.25"

866 ~~model's model~~ performance is consistent with the CNN model of Guo et al. (2021), demonstrating
867 its capability for reasonable/satisfactory flood depth estimates ~~under hurricane conditions.~~
868 However, when compared to the original model performance on Hurricane Ida, the R^2 values and
869 other metrics show weaker model performance for the transferability to other hurricanes,
870 suggesting reduced estimative accuracy, but not to the extent that the model performance becomes
871 unsatisfactory.

872 ~~Figure 6 presents the flood estimations for all four events. In both Hurricanes Ida and Irene,~~
873 ~~the model exhibited patterns of overestimation and underestimation across the study watershed.~~
874 ~~For Hurricanes Isaias and Sandy, we primarily observed overestimations, which may be attributed~~
875 ~~to their storm track locations. Furthermore, based on Figure 4, we mostly observe overestimation~~
876 ~~in shallower locations and underestimation for deeper water levels at the stream gauges. This~~
877 ~~pattern aligns with the southward total slope aspect, where the upper point of the river tends to~~
878 ~~have shallower depths and the mainstream exhibits deeper water levels.~~

879 ~~The model achieved an R^2~~ Figure 8 shows the relationship between observed and estimated
880 maximum water depths for the four storm events. Most observed water depths for the hurricanes
881 were low. For all four events, the data points suggested that the model tends to underestimate the
882 high water depths and overestimate the low water depths (Figure 8). The plots for Hurricanes
883 Sandy and Irene show a more dispersed set of points, suggesting a wider variance in the model
884 estimates compared to the observations. This implied that the model is less accurate in capturing

885 [the flood dynamics of these events or that these events have unique characteristics that are not](#)
886 [fully learned by the ML model.](#)



887

[Figure 8. Scatter plots of 0.80 for estimated vs observed flood depth for the four hurricanes.](#)
888 [For Hurricane Ida, our original model, 32% of the stream gauges had an \$F_0\$ between 90% to](#)
889 [110%, implying satisfactory estimates at these gauges \(Gallegos, Schubert, and Sanders 2012;](#)
890 [Gallegos, Schubert, and Sanders 2012;](#)

891 Schubert and Sanders 2012). Hurricanes Irene, scoring 0.77 for Isaias and 0.71 for Sandy and
892 Isaias had fewer gauges with moderate F_0 values of 16%, 14% and 3.5% out of all stream gauges
893 respectively, suggesting that the model estimations were less satisfactory for these events
894 compared to Ida in terms of bias. However, the transferability was still more successful for Irene
895 than the other two hurricanes, similar to what we found based on the other metrics (Table 4).

896 We attributed the model transferability performance to four main factors: water depth,
897 antecedent soil moisture, storm track and the primary driver of flooding. Based on tableTable 2,
898 Hurricanes Ida and Irene exhibited significant similarities in river water levels and antecedent soil
899 moisture. Given that river water level is the target variabledepths and antecedent soil moisture is
900 a crucial feature, which influenced their respective river water depths. These two hurricanes had
901 similar antecedent soil moisture conditions, while Hurricane Sandy had a higher antecedent soil
902 moisture percentage range of 17% to 38% compared to both Ida and Isaias, indicating a potentially
903 higher level of saturation before the storm arrival. These partly explain the better model
904 transferability for Hurricane Irene compared to Hurricanes Isaias and Sandy areis expected.

905 The spatial relationship betweenoriginal storm tracktrack of Hurricane Ida was located to the
906 watershed southeast, moving northeast, and remained fully outside the watershed locations also
907 plays a part in the model performance. Both Hurricanes Ida and Irene followed similar storm
908 tracks, located on the watershed's eastern side within a comparable distance range. In contrast,
909 Irene tracked were on the west side of (Figure 4). Hurricane Irene's path, which was somewhat
910 similar to Ida's, stretched from the southeast to the northeast, resulting in the best model
911 transferability. The key difference is that Irene's storm path lays inside the watershed, and
912 Hurricane Sandy was further south along its eastern border. Consequently, the model, assuming a
913 track similar to Ida's (the event that the model was trained for), underestimated maximum water

914 depths during Hurricane Irene. For Hurricanes Isaias and Sandy, which the storm track was farther
915 from the watershed. The model input feature "distance to storm track" played a and dissimilar from
916 Ida's path, the model overestimated the water depths. Isaias' storm track moved from the southwest
917 to the northwest of the watershed, while Sandy's unique path propagated from the southeast to the
918 southwest, leading to the lowest satisfactory in terms of the model transferability among the events.

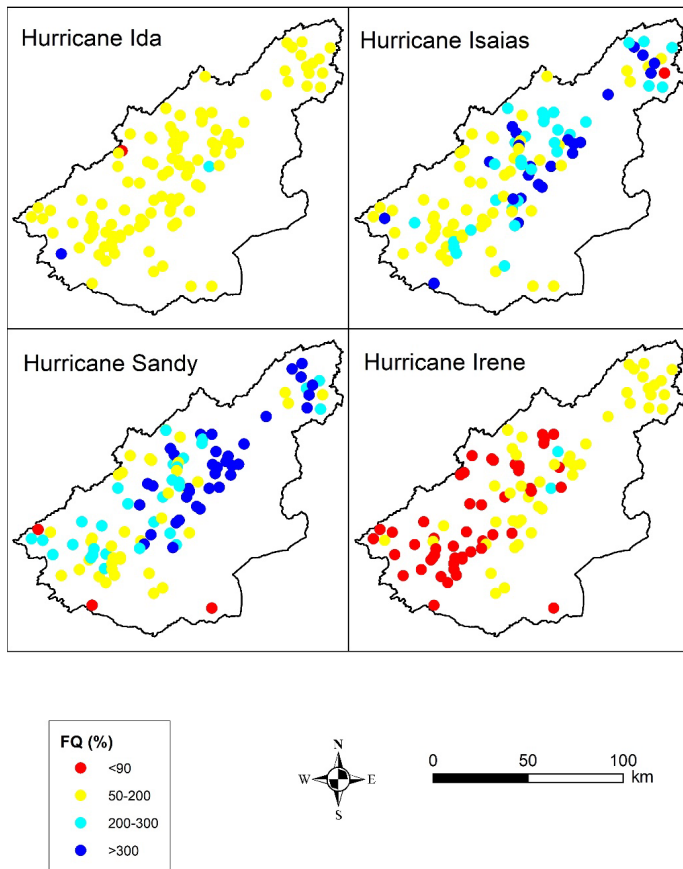
919 The other reason why the model transferability was most successful for Hurricane Irene was
920 that the event mainly driven by significant role, contributing to rainfall, similar to Hurricane Ida
921 (the event that the model was trained for). In contrast, the model performed worse for Hurricanes
922 Sandy and Isaias because these events were mainly driven by storm surge. The original model,
923 considered lower importance for storm surge, was not effective in predicting the water depths in
924 Sandy and Isaias. In fact, here we see another significant advantage of strategically using
925 physically meaningful features rather than the more commonly used black box approach. By
926 considering the physical phenomena in our model development, we can better transferability to
927 Hurricane Irene due to understand its similarity with hurricane Ida. However strengths and
928 weaknesses and more effectively evaluate its performance.

929 Despite these distinct characteristics of the storm events, the ML model ~~still~~ demonstrated
930 satisfactory performance on ~~Hurricane~~ Hurricanes Sandy and Isaias, suggesting some level of
931 transferability, mainly because we incorporated a wide array of pertinent flood influencing
932 features. ~~This sensitivity underscores the importance of training ML models on diverse hurricane~~
933 ~~trajectories and proximity to improve the model transferability, and the spatial dimension~~
934 (contributing watershed). While the model performs well, the inconsistency of the success level of
935 transferability across flood events presents opportunities to incorporate additional features or
936 training approaches, enhancing the model robustness to different storm tracks relative to the

937 watershed, and weighing the model features based on the main flood driver (e.g., rainfall or storm
938 surge).

939 The MAE values were higher for Hurricanes Sandy and Isaias, particularly when they were
940 farther away from the storm track. For instance, Hurricane Sandy had the highest MAE (1.69 m)
941 among the transferability cases, indicating larger estimation errors compared to the other
942 hurricanes. The model overestimated flood depths of Hurricanes Sandy and Isaias, while it
943 underestimated those during Hurricane Ida and Irene, likely due to their distance to the storm track.
944 Additionally, hurricanes Sandy and Isaias tend to yield higher F_Q values. For example, Hurricane
945 Sandy had the highest F_Q (366%), indicating larger discrepancies between the estimations and the
946 observed flood depths compared to Hurricanes Irene and Isaias.

947 These findings highlight the challenges of accurately hindcasting flood depths during more
948 severe hurricanes and underscore the importance of further refining the model to enhance its
949 performance in extreme events. Further investigations into the underlying features contributing to
950 these variations are crucial for improving flood hindcast models in the future. Insights gained from
951 this study can help develop transferable ML-based models that are computationally efficient for
952 flood hindcast.



953
954 **Figure 6: The ratio of estimated over-observed flood depth (F_Q) for the four hurricanes.**

955 **4.4. Limitations and future research**

956 While this study showed promising results about ML-based flood modeling, it is important to
 957 acknowledge its limitations to identify areas for future research. One significant limitation is the
 958 presence of inherent uncertainties in the model that can impact the accuracy of the estimations.
 959 These uncertainties can stem from various sources, including the quality and accuracy of the input

960 ~~data (features). For instance, relying solely on spatially aggregated values of features (mean and~~
961 ~~maximum used in this study) may not adequately capture the complex characteristics of the upper~~
962 ~~watershed. Future research should prioritize addressing these uncertainties by exploring alternative~~
963 ~~data sources and methodologies. The ANN model was tuned using observed flood data and a~~
964 ~~hyperparameter set was used as the optimal parameterization scenario. This deterministic approach~~
965 ~~does not incorporate the uncertainty from model parameterization. Probabilistic models are needed~~
966 ~~to address this uncertainty.~~

967 The study underscored the complexity of efficiently predicting water depths for major
968 hurricanes and emphasizes the necessity of refining models for better performance during such
969 extreme events. It highlighted the importance of deeper analyses into features causing prediction
970 discrepancies and suggested that addressing different flood types (fluvial vs. storm surge)
971 separately can enhance the model performance. This approach, alongside adjustments for specific
972 flood characteristics like storm tracks and similar influential factors that are distinct for each event,
973 can improve the performance of hindcast models, aiding in the development of more transferable
974 ML-based models.

976 **4.4. Limitations and future research**

977 While this study showed promising results about ML-based flood modeling, it is important to
978 acknowledge its limitations to identify areas for future research. One limitation is the presence of
979 inherent uncertainties in the model that can impact the accuracy of the estimations. These
980 uncertainties can stem from various sources, including the quality and accuracy of the observed
981 data (Merwade et al. 2008; Bales and Wagner 2009; Gallegos, Schubert, and Sanders 2012; Teng
982 et al. 2017) and input data (features). For instance, relying solely on spatially aggregated values of

983 features (mean and maximum used in this study) may not adequately capture the spatial
984 heterogeneity of pertinent variables across the upper watershed. Future research should prioritize
985 addressing these uncertainties by exploring alternative data sources and methodologies. The ANN-
986 MLP model was tuned using observed flood data and an optimal hyperparameter set was used
987 based on the hyperparameter optimization methods. This deterministic approach does not
988 incorporate the uncertainty from model parameterization. Probabilistic models are needed to
989 address this uncertainty. Parameterization uncertainty acknowledges that the exact values of model
990 parameters (e.g., weights in an ANN-MLP) determined through training may not perfectly capture
991 the true underlying processes, leading to variability in our predictions. Probabilistic models
992 address this uncertainty by incorporating it directly into the modeling process, offering a range of
993 possible outcomes with associated probabilities (posterior probability distributions) rather than a
994 single deterministic output. This is achieved through techniques like Bayesian inference, where
995 prior knowledge about parameters is updated with observed data to produce a posterior distribution
996 of parameters. This approach provides a more nuanced understanding of uncertainty, allowing
997 predictions to reflect both the variability observed in the data and the confidence in the model's
998 parameter estimates. To address the limitations of deterministic models, like the ANN-MLP used
999 in this study, future research should explore integrating probabilistic modeling techniques such as
1000 Bayesian inference. Exploring alternative data sources and methodologies, such as incorporating
1001 spatially detailed features or dynamic time series data, could also help in capturing the
1002 complexities of watershed characteristics more accurately.

1003 Furthermore, we did not have sub-daily data available for all ~~our~~ model features. Incorporating
1004 sub-daily data can highly likely improve the model accuracy in capturing intra-daily variability
1005 and flood dynamics, but it was not explored due to data constraints. Future research should

1006 incorporate sub-daily data into flood depth hindcast models. A further limitation of this study
1007 related to the time dimension is that wind events, storm surges, rainfall, and overland flow
1008 processes have different time signatures. Pluvial and storm surge flooding can be closely
1009 coincident with the storm event, but river ~~flood waves~~flood waves may take much longer to arrive
1010 at a particular location. The time lag between these processes was not considered in our ML model,
1011 which was not dynamic in time and only hindcasted maximum river ~~flood~~maximum water depths.
1012 Incorporating time-variability of the features can better represent the time-varying nature of flood
1013 dynamics.

1014 ~~Another limitation of this study is the issue of bathymetry and the need for further analyses to~~
1015 ~~incorporate better data in coastal watersheds. However, using DEMs without added bathymetry is~~
1016 ~~not entirely inaccurate, as they can already include bathymetry information in regions where~~
1017 ~~LiDAR can penetrate beneath clear water surfaces, particularly in rivers with low suspended~~
1018 ~~sediment and turbidity. On the other hand, coastal floods confined within riverbanks may heavily~~
1019 ~~depend on the main channel slope, while extreme events leading to flooding outside the channel~~
1020 ~~banks follow the general slope of floodplains and this is easily represented by DEMs without~~
1021 ~~considering underwater bathymetry.~~

1022 Another limitation of this study is the issue of bathymetry that is typically not represented well
1023 by DEMs like USGS' NED. Refining the DEMs with bathymetry data such as NOAA's
1024 Continuously Updated DEM (CUDEM) dataset and channel cross-sections is recommended to
1025 better represent the terrain on channels and floodplains in the model.

1026 Additionally, we modeled ~~flood~~maximum water depths across a large watershed (HUC6),
1027 whereby many details may not be important. For small watersheds and specially urbanized ones,
1028 we emphasize the importance of considering local factors such as sewer and drainage systems in

1029 flood depth hindcast, where pluvial floods may be prevalent. However, obtaining ~~comprehensive~~
1030 ~~and accurate~~ data on sewer and drainage systems can be challenging due to availability, lack of
1031 quality and confidentiality of the data, particularly at the desired spatial and temporal resolutions.
1032 Future research should strive to improve the availability and accessibility of such data to enhance
1033 the accuracy ~~and reliability~~ of flood depth hindcasting, especially in urban areas. In small urban
1034 watersheds, other details such as land management practices and other local features can also be
1035 important for flood depth hindcasting and should be incorporated in the ML-based model.

1036 This study primarily focused on hindcasting maximum ~~flood~~water depths and did not consider
1037 other important flood characteristics, such as ~~flood~~ duration, frequency, and extent, all of which
1038 are important for loss estimates, decision making and risk management (~~Ahmadisharaf and~~
1039 ~~Kalyanapu 2019; Kreibich et al. 2009; Merz et al. 2010; H. Qi and Altinakar 2011b; 2011a;~~
1040 ~~2012);(Ahmadisharaf and Kalyanapu 2019; Kreibich et al. 2009; Merz et al. 2010; Qi and~~
1041 ~~Altinakar 2011b; 2011a; 2012; Ebrahimian, Gulliver, and Wilson 2016; Ebrahimian et al. 2015).~~
1042 To gain a fuller picture of flood hazards, future research should aim to develop ML models that
1043 can hindcast these additional flood characteristics. We also focused on river ~~flood~~maximum water
1044 depths and did not hindcast inundation on floodplains- (~~out-of-channel~~). Developing ML-based
1045 models that can satisfactorily hindcast out-of-channel ~~flood~~maximum water depths should be a
1046 focus of future research; the transferability of ML-based models for such estimations should be
1047 also evaluated. High water marks (HWMs) can be used to train the model for such hindcasting.
1048 However, HWMs are subject to large uncertainties (Schubert et al. 2022). Therefore, one challenge
1049 in developing models that hindcast ~~flood~~maximum water depths over floodplains is the availability
1050 of reliable observations. Satellite-based observations are also often limited to flood status data;
1051 ~~flood~~maximum water depths cannot be estimated using these types of datasets. Newly launched

1052 satellites, such as the Surface Water and Ocean Topography (SWOT) mission, can provide
1053 additional data for such estimations.

1054 As part of future work, it is also essential to consider the sensitivity of stream gauges to changes
1055 in flow once water exceeds bankfull levels. This is significant as water height changes at a slower
1056 rate beyond bankfull due to the compound channel shape. Wide floodplains can lead to similar
1057 stage elevations for quite different flow conditions. This sensitivity assessment can offer insights
1058 about whether water levelsdepths can be estimated once flood conditions are established, which
1059 has implications for the model transferability across events.

1060 We recommend that future work compares the performance of our ML-based model to
1061 traditional physically-based and morphologic-based models using the same datasets. By evaluating
1062 the performance, generalizability, and computational efficiency of our ML-based model versus
1063 these traditional modeling approaches, we will be able to better validate the strengths of our data-
1064 driven methodology. Detailed error analyses between the approaches can also reveal insights into
1065 where additional physics knowledge needs to be incorporated into the ML-based model structure
1066 and training to improve performance.

1067 Thus, although we found ML-based models are transferable across flood events when informed
1068 by relevant physical features at meaningful locations, there are still several areas that require
1069 further investigations. By addressing these limitations, future research can corroborate our findings
1070 about the performance and transferability of ML-based models in estimating maximum floodwater
1071 depths as computationally-efficient modeling frameworks.

1072 5. Summary and conclusions

1073 This paper developed an ML-based model for hindcast maximum floodwater depths to address
1074 two major limitations of past research in applying ML models for flood estimations: solely

1075 predicting flood status (classification-based models) and debate on the transferability of these
1076 models across events. We used ANN-MLP to hindcast maximum floodwater depths over an event
1077 on a coastal watershed, which is affected by fluvial and tidal floods. The model was informed by
1078 underlying physical flood processes; and initial conditions (in the watershed and rivers),
1079 represented through a set of features (geographic location, topographic, climatic, land surface,
1080 hydrologic, hydrodynamic and soil). Unlike previous applications of ML algorithms, our model
1081 estimated floodmaximum water depths by accounting for the spatial distribution of the processes
1082 through considering both local contributions (at a given location) and those from the upstream
1083 watersheds. We demonstrated the model on a HUC6 watershed, Lower Hudson ~~Watershed~~, in the
1084 Northeastern United States and evaluated its transferability across major flood events—Hurricanes
1085 Ida, Sandy, Irene and Isaias. Feature selection techniques were used to identify the most influential
1086 features for flood hindcast. Hyperparameter optimization was performed to fine-tune the ML
1087 model, and its performance was evaluated using various metrics. The results showed that the model
1088 performed satisfactorily in estimating maximum floodwater depths for the original event,
1089 Hurricane Ida ($R^2 = 0.9294$, MAE= 0.6664 meters, MDAE= 0.45 meters, NRMSE= 2924%, and
1090 $F_Q = 139138\%$). The model transferability (i.e., applying the validated model as is without any
1091 additional parameter tuning) within the same watershed against three other events showed that the
1092 developed model was promising in the estimations ($R^2 > 0.747$, MAE < 1.6971 meters, MDAE <
1093 1.78 meters, NRMSE < 109%, and $F_Q < 366370\%$). This showed the model ability to capture
1094 complex relationships between the maximum flood depth and pertinent features beyond what it
1095 was originally trained for. Future research is needed to further evaluate the transferability of ML
1096 models across events and watersheds with different drainage areas for flood depth estimations.

1097 Code availability

1098 The ML codes accessible at GitHub: ([https://github.com/mpakdehi/ANN_MLP-flood-depth-](https://github.com/mpakdehi/ANN_MLP-flood-depth-model)
1099 model).

1100 Data availability

1101 All the data are public domain and can be acquired from online repositories.

1102 **Author contribution**

1103 **MP:** Data curation, Formal analysis, Investigation, Methodology, Software, Validation,
1104 Visualization, Writing – original draft preparation; **EA:** Conceptualization, Methodology, Funding
1105 acquisition, Project administration, Supervision, Writing – review & editing; **BN:** Methodology,
1106 Writing – review & editing; **EC:** Visualization, Writing – review & editing.

1107 ~~Code availability~~

1108 ~~The ML codes can be shared upon request.~~

1109 ~~Data availability~~

1110 ~~All the data are public domain and can be acquired from online repositories.~~

1111 **Competing interests**

1112 The ~~contact author has declared~~authors declare that ~~none~~they have no conflict of ~~the authors has~~
1113 ~~any competing interests~~interest.

1114 **Acknowledgements**

1115 This study was partially supported through a research grant by United States' National Science
1116 Foundation (award number 2203180). We thank Paul Bates for the detailed review and fruitful
1117 comments on this manuscript.

1118 **References**

- 1119 ~~Abdollahi, Abolfazl, and Biswajeet Pradhan. 2021. "Urban Vegetation Mapping from Aerial~~
1120 ~~Imagery Using Explainable AI (XAI)." *Sensors* 21 (14): 4738.~~
1121 ~~<https://doi.org/10.3390/s21144738>.~~
- 1122 ~~Abdrabo, Karim I., Sameh A. Kantoush, Aly Esmail, Mohamed Saber, Tetsuya Sumi, Mahmood~~
1123 ~~Almamari, Bahaa Elboshy, and Safaa Ghoniem. 2023. "An Integrated Indicator Based~~
1124 ~~Approach for Constructing an Urban Flood Vulnerability Index as an Urban Decision-~~
1125 ~~Making Tool Using the PCA and AHP Techniques: A Case Study of Alexandria, Egypt."~~
1126 ~~*Urban Climate* 48 (March): 101426. <https://doi.org/10.1016/j.uelim.2023.101426>.~~
- 1127 ~~Abraham, Robert, P. E. Kneale, and Linda M. See. 2004. *Neural Networks for Hydrological*~~
1128 ~~*Modeling*. CRC Press.~~
- 1129 ~~Adamowski, Jan, Hiu Fung Chan, Shiv O. Prasher, and Vishwa Nath Sharda. 2011. "Comparison~~
1130 ~~of Multivariate Adaptive Regression Splines with Coupled Wavelet Transform Artificial~~
1131 ~~Neural Networks for Runoff Forecasting in Himalayan Micro Watersheds with Limited~~
1132 ~~Data." *Journal of Hydroinformatics* 14 (3): 731-44.~~
1133 ~~<https://doi.org/10.2166/hydro.2011.044>.~~
- 1134 ~~Adedeji, Itunu C., Ebrahim Ahmadisharaf, and Yanshuo Sun. 2022. "Predicting In-Stream Water~~
1135 ~~Quality Constituents at the Watershed Scale Using Machine Learning." *Journal of*~~
1136 ~~*Contaminant Hydrology* 251 (December): 104078.~~
1137 ~~<https://doi.org/10.1016/j.jconhyd.2022.104078>.~~
- 1138 ~~Ahmadisharaf Ebrahim, Camacho René A., Zhang Harry X., Hantush Mohamed M., and~~
1139 ~~Mohamoud Yusuf M. 2019. "Calibration and Validation of Watershed Models and~~

1140 Advances in Uncertainty Analysis in TMDL Studies.” *Journal of Hydrologic Engineering*
1141 24 (7): 03119001. [https://doi.org/10.1061/\(ASCE\)HE.1943-5584.0001794](https://doi.org/10.1061/(ASCE)HE.1943-5584.0001794).

1142 Ahmadisharaf, Ebrahim, and Alfred J Kalyanapu. 2019. “A Coupled Probabilistic Hydrologic and
1143 Hydraulic Modelling Framework to Investigate the Uncertainty of Flood Loss Estimates.”
1144 *Journal of Flood Risk Management* 12 (S2): e12536. <https://doi.org/10.1111/jfr3.12536>.

1145 Ahmadisharaf, Ebrahim, Alfred J. Kalyanapu, Brantley A. Thames, and Jason Lillywhite. 2016.
1146 “A Probabilistic Framework for Comparison of Dam Breach Parameters and Outflow
1147 Hydrograph Generated by Different Empirical Prediction Methods.” *Environmental*
1148 *Modelling & Software* 86 (December): 248–63.
1149 <https://doi.org/10.1016/j.envsoft.2016.09.022>.

1150 Anderson, Tiffany R., Charles H. Fletcher, Matthew M. Barbee, Bradley M. Romine, Sam Lemmo,
1151 and Jade M. S. Delevaux. 2018. “Modeling Multiple Sea Level Rise Stresses Reveals up
1152 to Twice the Land at Risk Compared to Strictly Passive Flooding Methods.” *Scientific*
1153 *Reports* 8 (1): 14484. <https://doi.org/10.1038/s41598-018-32658-x>.

1154 Bafitlhile, Thabo Michael, and Zhijia Li. 2019. “Applicability of ϵ -Support Vector Machine and
1155 Artificial Neural Network for Flood Forecasting in Humid, Semi-Humid and Semi-Arid
1156 Basins in China.” *Water* 11 (1): 85. <https://doi.org/10.3390/w11010085>.

1157 Bates, Paul D. 2022. “Flood Inundation Prediction.” *Annual Review of Fluid Mechanics* 54 (1):
1158 287–315. <https://doi.org/10.1146/annurev-fluid-030121-113138>.

1159 Bates, Paul D., Richard J. Dawson, Jim W. Hall, Matthew S. Horritt, Robert J. Nicholls, Jon Wicks,
1160 and Mohamed Ahmed Ali Mohamed Hassan. 2005. “Simplified Two-Dimensional
1161 Numerical Modelling of Coastal Flooding and Example Applications.” *Coastal*
1162 *Engineering* 52 (9): 793–810. <https://doi.org/10.1016/j.coastaleng.2005.06.001>.

- 1163 ~~Bentivoglio, Roberto, Elvin Isufi, Sebastian Nicolaas Jonkman, and Riccardo Taormina. 2022.~~
1164 ~~“Deep Learning Methods for Flood Mapping: A Review of Existing Applications and~~
1165 ~~Future Research Directions.” *Hydrology and Earth System Sciences* 26 (16): 4345–78.~~
1166 ~~<https://doi.org/10.5194/hess-26-4345-2022>.~~
- 1167 ~~Berkhahn, Simon, Lothar Fuchs, and Insa Neuweiler. 2019. “An Ensemble Neural Network Model~~
1168 ~~for Real Time Prediction of Urban Floods.” *Journal of Hydrology* 575 (August): 743–54.~~
1169 ~~<https://doi.org/10.1016/j.jhydrol.2019.05.066>.~~
- 1170 ~~Beven H, John L., Andrew Hagen, and Robbie Berg. 2022. “Tropical Cyclone Report—~~
1171 ~~HURRICANE IDA (AL092021).” National Hurricane Center. April 4, 2022.~~
1172 ~~https://www.nhc.noaa.gov/data/ter/AL092021_Ida.pdf.~~
- 1173 ~~Beven, K. J., and M. J. Kirkby. 1979. “A Physically Based, Variable-Contributing Area Model of~~
1174 ~~Basin Hydrology / Un Modèle à Base Physique de Zone d’appel Variable de l’hydrologie~~
1175 ~~Du Bassin Versant.” *Hydrological Sciences Bulletin* 24 (1): 43–69.~~
1176 ~~<https://doi.org/10.1080/02626667909491834>.~~
- 1177 ~~Bhuyian, Md N. M., and Alfred Kalyanapu. 2020. “Predicting Channel Conveyance and~~
1178 ~~Characterizing Planform Using River Bathymetry via Satellite Image Compilation~~
1179 ~~(RiBaSIC) Algorithm for DEM-Based Hydrodynamic Modeling.” *Remote Sensing* 12 (17):~~
1180 ~~2799. <https://doi.org/10.3390/rs12172799>.~~
- 1181 ~~Blake, Eric S., Todd B. Kimberlain, Robert J. Berg, John P. Cangialosi, and John L. Beven H.~~
1182 ~~2013. “Tropical Cyclone Report—Hurricane Sandy (AL182012).” National Hurricane~~
1183 ~~Center. February 12, 2013. https://www.nhc.noaa.gov/data/ter/AL182012_Sandy.pdf.~~

- 1184 Boulouard, Zakaria, Mariyam Ouaisa, Mariya Ouaisa, Farhan Siddiqui, Mutiq Almutiq, and
1185 Moez Kriehen. 2022. "An Integrated Artificial Intelligence of Things Environment for
1186 River Flood Prevention." *Sensors* 22 (23): 9485. <https://doi.org/10.3390/s22239485>.
- 1187 Cao, Yifan, Hongliang Jia, Junnan Xiong, Weiming Cheng, Kun Li, Quan Pang, and Zhiwei Yong.
1188 2020. "Flash Flood Susceptibility Assessment Based on Geodetector, Certainty Factor, and
1189 Logistic Regression Analyses in Fujian Province, China." *ISPRS International Journal of*
1190 *Geo-Information* 9 (12): 748. <https://doi.org/10.3390/ijgi9120748>.
- 1191 Chang, Li Chiu, Jia Yi Liou, and Fi John Chang. 2022. "Spatial Temporal Flood Inundation
1192 Nowcasts by Fusing Machine Learning Methods and Principal Component Analysis." *Journal*
1193 *of Hydrology* 612 (September): 128086.
1194 <https://doi.org/10.1016/j.jhydrol.2022.128086>.
- 1195 Chen, Yuguo, Xinyi Zhang, Kejun Yang, Shiyi Zeng, and Anyu Hong. 2023. "Modeling Rules of
1196 Regional Flash Flood Susceptibility Prediction Using Different Machine Learning
1197 Models." *Frontiers in Earth Science* 11.
1198 <https://www.frontiersin.org/articles/10.3389/feart.2023.1117004>.
- 1199 Costabile, Pierfranco, Carmelina Costanzo, and Francesco Macchione. 2017. "Performances and
1200 Limitations of the Diffusive Approximation of the 2-d Shallow Water Equations for Flood
1201 Simulation in Urban and Rural Areas." *Applied Numerical Mathematics, New Trends in*
1202 *Numerical Analysis: Theory, Methods, Algorithms and Applications (NETNA 2015)*, 116
1203 (June): 141–56. <https://doi.org/10.1016/j.apnum.2016.07.003>.
- 1204 Davenport, Frances V., Marshall Burke, and Noah S. Diffenbaugh. 2021. "Contribution of
1205 Historical Precipitation Change to US Flood Damages." *Proceedings of the National*
1206 *Academy of Sciences* 118 (4): e2017524118. <https://doi.org/10.1073/pnas.2017524118>.

1207 Dawson, C. W., R. J. Abrahart, A. Y. Shamseldin, and R. L. Wilby. 2006. "Flood Estimation at
1208 Ungauged Sites Using Artificial Neural Networks." *Journal of Hydrology* 319 (1): 391–
1209 409. <https://doi.org/10.1016/j.jhydrol.2005.07.032>.

1210 Elkhrachy, Ismail. 2022. "Flash Flood Water Depth Estimation Using SAR Images, Digital
1211 Elevation Models, and Machine Learning Algorithms." *Remote Sensing* 14 (3): 440.
1212 <https://doi.org/10.3390/rs14030440>.

1213 Fernández Pato, Javier, Daniel Caviedes-Voullième, and Pilar García-Navarro. 2016.
1214 "Rainfall/Runoff Simulation with 2D Full Shallow Water Equations: Sensitivity Analysis
1215 and Calibration of Infiltration Parameters." *Journal of Hydrology* 536 (May): 496–513.
1216 <https://doi.org/10.1016/j.jhydrol.2016.03.021>.

1217 Galloway, Gerald E, Allison Reilly, Sung Ryoo, Anjanette Riley, Maggie Haslam, Sam Brody,
1218 Wesley Highfield, Joshua Goldstein, Jayton Rainey, and Sherry Parker,. 2018. "Urban
1219 Flooding Report Online.Pdf." THE GROWING THREAT OF URBAN FLOODING: A
1220 NATIONAL CHALLENGE. 2018. [https://today.tamu.edu/wp-](https://today.tamu.edu/wp-content/uploads/sites/4/2018/11/Urban-flooding-report-online.pdf)
1221 [content/uploads/sites/4/2018/11/Urban-flooding-report-online.pdf](https://today.tamu.edu/wp-content/uploads/sites/4/2018/11/Urban-flooding-report-online.pdf).

1222 Gray W. Brunner. 2016. "HEC RAS, River Analysis System Hydraulic Reference Manual."
1223 February 2016. [https://www.hec.usace.army.mil/software/hec-ras/documentation/HEC-](https://www.hec.usace.army.mil/software/hec-ras/documentation/HEC-RAS%205.0%20Reference%20Manual.pdf)
1224 [RAS%205.0%20Reference%20Manual.pdf](https://www.hec.usace.army.mil/software/hec-ras/documentation/HEC-RAS%205.0%20Reference%20Manual.pdf).

1225 Gudiyangada Nachappa, Thimmaiah, Sepideh Tavakkoli Piralilou, Khalil Gholamnia, Omid
1226 Ghorbanzadeh, Omid Rahmati, and Thomas Blaschke. 2020. "Flood Susceptibility
1227 Mapping with Machine Learning, Multi-Criteria Decision Analysis and Ensemble Using
1228 Dempster Shafer Theory." *Journal of Hydrology* 590 (November): 125275.
1229 <https://doi.org/10.1016/j.jhydrol.2020.125275>.

1230 Guo, Zifeng, João P. Leitão, Nuno E. Simões, and Vahid Moosavi. 2021. "Data Driven Flood
1231 Emulation: Speeding up Urban Flood Predictions by Deep Convolutional Neural
1232 Networks." *Journal of Flood Risk Management* 14 (1): e12684.
1233 <https://doi.org/10.1111/jfr3.12684>.

1234 Hashmi, Farukh. 2020. "How to Tune Hyperparameters Using Random Search CV in Python." *Thinking Neuron* (blog). September 10, 2020. <https://thinkingneuron.com/how-to-tune-hyperparameters-using-random-search-cv-in-python/>.

1237 Hemmati, Mona, Bruce R. Ellingwood, and Hussam N. Mahmoud. 2020. "The Role of Urban
1238 Growth in Resilience of Communities Under Flood Risk." *Earth's Future* 8 (3).
1239 <https://doi.org/10.1029/2019EF001382>.

1240 Hino, Miyuki, and Earthea Nance. 2021. "Five Ways to Ensure Flood Risk Research Helps the
1241 Most Vulnerable." *Nature* 595 (7865): 27–29. <https://doi.org/10.1038/d41586-021-01750-0>.

1242 0.

1243 Hosseini, Farzaneh Sajedi, Bahram Choubin, Amir Mosavi, Narjes Nabipour, Shahaboddin
1244 Shamsirband, Hamid Darabi, and Ali Torabi Haghighi. 2020. "Flash Flood Hazard
1245 Assessment Using Ensembles and Bayesian Based Machine Learning Models: Application
1246 of the Simulated Annealing Feature Selection Method." *Science of The Total Environment*
1247 711 (April): 135161. <https://doi.org/10.1016/j.scitotenv.2019.135161>.

1248 Hosseiny, Hossein, Foad Nazari, Virginia Smith, and C. Nataraj. 2020. "A Framework for
1249 Modeling Flood Depth Using a Hybrid of Hydraulics and Machine Learning." *Scientific
1250 Reports* 10 (1): 8222. <https://doi.org/10.1038/s41598-020-65232-5>.

1251 Hu, Anson, and Ibrahim Demir. 2021. "Real Time Flood Mapping on Client Side Web Systems
1252 Using HAND Model." *Hydrology* 8 (2): 65. <https://doi.org/10.3390/hydrology8020065>.

1253 ~~Huang, Faming, Siyu Tao, Deying Li, Zhipeng Lian, Filippo Catani, Jinsong Huang, Kailong Li,~~
1254 ~~and Chuhong Zhang. 2022. "Landslide Susceptibility Prediction Considering~~
1255 ~~Neighborhood Characteristics of Landslide Spatial Datasets and Hydrological Slope Units~~
1256 ~~Using Remote Sensing and GIS Technologies." *Remote Sensing* 14 (18): 4436.~~
1257 ~~<https://doi.org/10.3390/rs14184436>.~~

1258 ~~Jafarzadegan, Keighobad, and Venkatesh Merwade. 2019. "Probabilistic Floodplain Mapping~~
1259 ~~Using HAND-Based Statistical Approach." *Geomorphology* 324 (January): 48–61.~~
1260 ~~<https://doi.org/10.1016/j.geomorph.2018.09.024>.~~

1261 ~~Jafarzadegan, Keighobad, Hamid Moradkhani, Florian Pappenberger, Hamed Moftakhari, Paul~~
1262 ~~Bates, Peyman Abbaszadeh, Reza Marsooli, et al. 2023. "Recent Advances and New~~
1263 ~~Frontiers in Riverine and Coastal Flood Modeling." *Reviews of Geophysics* 61 (2):~~
1264 ~~e2022RG000788. <https://doi.org/10.1029/2022RG000788>.~~

1265 ~~Joseph, V. Roshan. 2022. "Optimal Ratio for Data Splitting." *Statistical Analysis and Data*~~
1266 ~~*Mining: The ASA Data Science Journal* 15 (4): 531–38.~~
1267 ~~<https://doi.org/10.1002/sam.11583>.~~

1268 ~~Kalyanapu, Alfred J., Siddharth Shankar, Eric R. Pardyjak, David R. Judi, and Steven J. Burian.~~
1269 ~~2011. "Assessment of GPU Computational Enhancement to a 2D Flood Model."~~
1270 ~~*Environmental Modelling & Software* 26 (8): 1009–16.~~
1271 ~~<https://doi.org/10.1016/j.envsoft.2011.02.014>.~~

1272 ~~Khosravi, Khabat, Binh Thai Pham, Kamran Chapi, Ataollah Shirzadi, Himan Shahabi, Inge~~
1273 ~~Revhaug, Indra Prakash, and Dieu Tien Bui. 2018. "A Comparative Assessment of~~
1274 ~~Decision Trees Algorithms for Flash Flood Susceptibility Modeling at Haraz Watershed,~~

1275 Northern Iran.” *Science of The Total Environment* 627 (June): 744–55.
1276 <https://doi.org/10.1016/j.scitotenv.2018.01.266>.

1277 Kim, Sooyoul, Yoshiharu Matsumi, Shunqi Pan, and Hajime Mase. 2016. “A Real-Time Forecast
1278 Model Using Artificial Neural Network for after Runner Storm Surges on the Tottori
1279 Coast, Japan.” *Ocean Engineering* 122 (August): 44–53.
1280 <https://doi.org/10.1016/j.oceaneng.2016.06.017>.

1281 Kratzert, Frederik, Daniel Klotz, Mathew Herrnegger, Alden K. Sampson, Sepp Hochreiter, and
1282 Grey S. Nearing. 2019. “Toward Improved Predictions in Ungauged Basins: Exploiting the
1283 Power of Machine Learning.” *Water Resources Research* 55 (12): 11344–54.
1284 <https://doi.org/10.1029/2019WR026065>.

1285 Kreibich, H., K. Piroth, I. Seifert, H. Maiwald, U. Kunert, J. Schwarz, B. Merz, and A. H. Thielen.
1286 2009. “Is Flow Velocity a Significant Parameter in Flood Damage Modelling?” *Natural
1287 Hazards and Earth System Sciences* 9 (5): 1679–92. [https://doi.org/10.5194/nhess-9-1679-](https://doi.org/10.5194/nhess-9-1679-2009)
1288 [2009](https://doi.org/10.5194/nhess-9-1679-2009).

1289 Kulp, Scott A., and Benjamin H. Strauss. 2019. “New Elevation Data Triple Estimates of Global
1290 Vulnerability to Sea Level Rise and Coastal Flooding.” *Nature Communications* 10 (1):
1291 4844. <https://doi.org/10.1038/s41467-019-12808-z>.

1292 Kundzewicz, ZW, Buda Su, Yanjun Wang, Jun Xia, Jinlong Huang, and Tong Jiang. 2019. “Flood
1293 Risk and Its Reduction in China.” *Advances in Water Resources* 130 (August): 37–45.
1294 <https://doi.org/10.1016/j.advwatres.2019.05.020>.

1295 Latto, Andy, Andrew Hagen, and Robbie Berg. 2021. “Tropical Cyclone Report—HURRICANE
1296 ISAIAS (AL092020).” National Hurricane Center. June 11, 2021.
1297 https://www.nhc.noaa.gov/data/ter/AL092020_Isaias.pdf.

1298 Lee, Deuk Hwan, Yun Tae Kim, and Seung Rae Lee. 2020. "Shallow Landslide Susceptibility
1299 Models Based on Artificial Neural Networks Considering the Factor Selection Method and
1300 Various Non-Linear Activation Functions." *Remote Sensing* 12 (7): 1194.
1301 <https://doi.org/10.3390/rs12071194>.

1302 Lixion A., Avila, and John Cangialosi. 2013. "Tropical Cyclone Report—Hurricane Irene
1303 (AL092011)." National Hurricane Center. April 11, 2013.
1304 https://www.nhc.noaa.gov/data/ter/AL092011_Irene.pdf.

1305 Löwe, Roland, Julian Böhm, David Getreuer Jensen, Jorge Leandro, and Soren Hojmark
1306 Rasmussen. 2021. "U FLOOD—Topographic Deep Learning for Predicting Urban Pluvial
1307 Flood Water Depth." *Journal of Hydrology* 603 (December): 126898.
1308 <https://doi.org/10.1016/j.jhydrol.2021.126898>.

1309 Lundberg, Scott, and Su In Lee. 2017. "A Unified Approach to Interpreting Model Predictions."
1310 arXiv. <http://arxiv.org/abs/1705.07874>.

1311 Maier, Holger R., Stefano Galelli, Saman Razavi, Andrea Castelletti, Andrea Rizzoli, Ioannis N.
1312 Athanasiadis, Miquel Sánchez-Marrè, Marco Acutis, Wenyang Wu, and Greer B.
1313 Humphrey. 2023. "Exploding the Myths: An Introduction to Artificial Neural Networks
1314 for Prediction and Forecasting." *Environmental Modelling & Software* 167 (September):
1315 105776. <https://doi.org/10.1016/j.envsoft.2023.105776>.

1316 McCulloch, Warren S., and Walter Pitts. 1943. "A Logical Calculus of the Ideas Immanent in
1317 Nervous Activity." *The Bulletin of Mathematical Biophysics* 5 (4): 115–33.
1318 <https://doi.org/10.1007/BF02478259>.

- 1319 Merz, B, Heidi Kreibich, R-Schwarze, and Annette Thielen. 2010. "Review Article" Assessment
1320 of Economic Flood Damage." *Natural Hazards and Earth System Sciences* 10: 1697–
1321 1724. <https://doi.org/10.5194/nhess-10-1697-2010>.
- 1322 Ming, Xiaodong, Qiuhua Liang, Xilin Xia, Dingmin Li, and Hayley J. Fowler. 2020. "Real Time
1323 Flood Forecasting Based on a High Performance 2-D Hydrodynamic Model and
1324 Numerical Weather Predictions." *Water Resources Research* 56 (7): e2019WR025583.
1325 <https://doi.org/10.1029/2019WR025583>.
- 1326 Mishra, Ashok, Sourav Mukherjee, Bruno Merz, Vijay P. Singh, Daniel B. Wright, Villarini
1327 Gabriele, Subir Paul, et al. 2022. "An Overview of Flood Concepts, Challenges, and Future
1328 Directions." *Journal of Hydrologic Engineering* 27 (6).
1329 [https://ascelibrary.org/doi/full/10.1061/\(ASCE\)HE.1943-5584.0002164](https://ascelibrary.org/doi/full/10.1061/(ASCE)HE.1943-5584.0002164).
- 1330 Mosavi, Amir, Pinar Ozturk, and Kwok wing Chau. 2018. "Flood Prediction Using Machine
1331 Learning Models: Literature Review." *Water* 10 (11): 1536.
1332 <https://doi.org/10.3390/w10111536>.
- 1333 National Academies of Sciences, Engineering, and Medicine. 2019. *Framing the Challenge of
1334 Urban Flooding in the United States*. Washington, DC: The National Academies Press.
1335 <https://doi.org/10.17226/25381>.
- 1336 National Hurricane Center. 2022. "National Hurricane Center." 2022.
1337 <https://www.nhc.noaa.gov/index.shtml>.
- 1338 Nguyen, Quang Hung, Hai Bang Ly, Lanh Si Ho, Nakhir Al-Ansari, Hiep Van Le, Van Quan Tran,
1339 Indra Prakash, and Binh Thai Pham. 2021. "Influence of Data Splitting on Performance of
1340 Machine Learning Models in Prediction of Shear Strength of Soil." *Mathematical*

1341 ~~*Problems in Engineering* 2021 (February): e4832864.~~
1342 ~~<https://doi.org/10.1155/2021/4832864>.~~
1343 ~~“NOAA Tides & Currents.” 2023. CO OPS Map NOAA Tides & Currents. 2023.~~
1344 ~~<https://tidesandcurrents.noaa.gov/map/index.html>.~~
1345 ~~NOAA’s NCEI. 2022. “Data Search | National Centers for Environmental Information (NCEI).”~~
1346 ~~2022. <https://www.ncei.noaa.gov/access/search/data-search/local-climatological-data>.~~
1347 ~~Pham, Binh Thai, Chinh Luu, Tran Van Phong, Phan Trong Trinh, Ataollah Shirzadi, Somayeh~~
1348 ~~Renoud, Shahrokh Asadi, Hiep Van Le, Jason von Meding, and John J. Clague. 2021. “Can~~
1349 ~~Deep Learning Algorithms Outperform Benchmark Machine Learning Algorithms in~~
1350 ~~Flood Susceptibility Modeling?” *Journal of Hydrology* 592 (January): 125615.~~
1351 ~~<https://doi.org/10.1016/j.jhydrol.2020.125615>.~~
1352 ~~Pradhan, Biswajeet. 2009. “Journal of Spatial Hydrology Vol.9, No.2 Fall 2009.”~~
1353 ~~Qi, Honghai, and Mustafa S. Altinakar. 2011a. “A Conceptual Framework of Agricultural Land~~
1354 ~~Use Planning with BMP for Integrated Watershed Management.” *Journal of*~~
1355 ~~*Environmental Management* 92 (1): 149–55.~~
1356 ~~<https://doi.org/10.1016/j.jenvman.2010.08.023>.~~
1357 ~~. 2011b. “Vegetation Buffer Strips Design Using an Optimization Approach for Non-Point~~
1358 ~~Source Pollutant Control of an Agricultural Watershed.” *Water Resources Management* 25~~
1359 ~~(2): 565–78. <https://doi.org/10.1007/s11269-010-9714-9>.~~
1360 ~~. 2012. “GIS Based Decision Support System for Dam Break Flood Management under~~
1361 ~~Uncertainty with Two Dimensional Numerical Simulations.” *Journal of Water Resources*~~
1362 ~~*Planning and Management* 138 (4): 334–41. [https://doi.org/10.1061/\(ASCE\)WR.1943-](https://doi.org/10.1061/(ASCE)WR.1943-5452.0000192)~~
1363 ~~[5452.0000192](https://doi.org/10.1061/(ASCE)WR.1943-5452.0000192).~~

- 1364 Qi, Wenchao, Chao Ma, Hongshi Xu, Zifan Chen, Kai Zhao, and Hao Han. 2021. "A Review on
1365 Applications of Urban Flood Models in Flood Mitigation Strategies." *Natural Hazards* 108
1366 (1): 31–62. <https://doi.org/10.1007/s11069-021-04715-8>.
- 1367 Rafiei-Sardooi, Elham, Ali Azareh, Bahram Choubin, Amir H. Mosavi, and John J. Clague. 2021.
1368 "Evaluating Urban Flood Risk Using Hybrid Method of TOPSIS and Machine Learning." *2*
1369 *International Journal of Disaster Risk Reduction* 66 (December): 102614.
1370 <https://doi.org/10.1016/j.ijdrr.2021.102614>.
- 1371 Rahmati, Omid, Hamid Reza Pourghasemi, and Hossein Zeinivand. 2016. "Flood Susceptibility
1372 Mapping Using Frequency Ratio and Weights of Evidence Models in the Golastan
1373 Province, Iran." *Geocarto International* 31 (1): 42–70.
1374 <https://doi.org/10.1080/10106049.2015.1041559>.
- 1375 Reekien, Diana. 2018. "What Is in an Index? Construction Method, Data Metric, and Weighting
1376 Scheme Determine the Outcome of Composite Social Vulnerability Indices in New York
1377 City." *Regional Environmental Change* 18 (5): 1439–51. [https://doi.org/10.1007/s10113-](https://doi.org/10.1007/s10113-017-1273-7)
1378 [017-1273-7](https://doi.org/10.1007/s10113-017-1273-7).
- 1379 Rennó, Camilo Daleles, Antonio Donato Nobre, Luz Adriana Cuartas, João Vianei Soares, Martin
1380 G. Hodnett, Javier Tomasella, and Maarten J. Waterloo. 2008. "HAND, a New Terrain
1381 Descriptor Using SRTM-DEM: Mapping Terra Firme Rainforest Environments in
1382 Amazonia." *Remote Sensing of Environment* 112 (9): 3469–81.
1383 <https://doi.org/10.1016/j.rse.2008.03.018>.
- 1384 Rezaie, Fatemeh, Mahdi Panahi, Sayed M. Bateni, Changhyun Jun, Christopher M. U. Neale, and
1385 Saro Lee. 2022. "Novel Hybrid Models by Coupling Support Vector Regression (SVR)

1386 with Meta-Heuristic Algorithms (WOA and GWO) for Flood Susceptibility Mapping.”
1387 *Natural Hazards* 114 (2): 1247–83. <https://doi.org/10.1007/s11069-022-05424-6>.

1388 Rumelhart, David E., James L. McClelland, and PDP Research Group. 1986. *Parallel Distributed*
1389 *Processing: Explorations in the Microstructure of Cognition: Foundations*. The MIT
1390 Press. <https://doi.org/10.7551/mitpress/5236.001.0001>.

1391 Salvati, Aryan, Alireza Moghaddam Nia, Ali Salajegheh, Kayvan Ghaderi, Dawood Talebpour
1392 Asl, Nadhir Al-Ansari, Feridon Solaimani, and John J. Clague. 2023. “Flood Susceptibility
1393 Mapping Using Support Vector Regression and Hyper-Parameter Optimization.” *Journal*
1394 *of Flood Risk Management* n/a (n/a): e12920. <https://doi.org/10.1111/jfr3.12920>.

1395 Schubert, Jochen E., Adam Luke, Amir AghaKouchak, and Brett F. Sanders. 2022. “A Framework
1396 for Mechanistic Flood Inundation Forecasting at the Metropolitan Scale.” *Water Resources*
1397 *Research* 58 (10): e2021WR031279. <https://doi.org/10.1029/2021WR031279>.

1398 Schubert, Jochen E., and Brett F. Sanders. 2012. “Building Treatments for Urban Flood Inundation
1399 Models and Implications for Predictive Skill and Modeling Efficiency.” *Advances in Water*
1400 *Resources* 41 (June): 49–64. <https://doi.org/10.1016/j.advwatres.2012.02.012>.

1401 Sridhar, Venkataramana, Syed Azhar Ali, and David J. Sample. 2021. “Systems Analysis of
1402 Coupled Natural and Human Processes in the Mekong River Basin.” *Hydrology* 8 (3): 140.
1403 <https://doi.org/10.3390/hydrology8030140>.

1404 Stow, Craig A., Chris Roessler, Mark E. Borsuk, James D. Bowen, and Kenneth H. Reckhow.
1405 2003. “Comparison of Estuarine Water Quality Models for Total Maximum Daily Load
1406 Development in Neuse River Estuary.” *Journal of Water Resources Planning and*
1407 *Management* 129 (4): 307–14. [https://doi.org/10.1061/\(ASCE\)0733-](https://doi.org/10.1061/(ASCE)0733-9496(2003)129:4(307))
1408 [9496\(2003\)129:4\(307\)](https://doi.org/10.1061/(ASCE)0733-9496(2003)129:4(307)).

1409 Sun, Deliang, Jiahui Xu, Haijia Wen, and Yue Wang. 2020. "An Optimized Random Forest Model
1410 and Its Generalization Ability in Landslide Susceptibility Mapping: Application in Two
1411 Areas of Three Gorges Reservoir, China." *Journal of Earth Science* 31 (6): 1068–86.
1412 <https://doi.org/10.1007/s12583-020-1072-9>.

1413 USGS. 2022. "TNM Download V2." 2022. <https://apps.nationalmap.gov/downloader/>.

1414 Viglione, Alberto, Giuliano Di Baldassarre, Luigia Brandimarte, Linda Kuil, Gemma Carr, José
1415 Luis Salinas, Anna Scolobig, and Günter Blöschl. 2014. "Insights from Socio-Hydrology
1416 Modelling on Dealing with Flood Risk—Roles of Collective Memory, Risk Taking
1417 Attitude and Trust." *Journal of Hydrology, Creating Partnerships Between Hydrology and
1418 Social Science: A Priority for Progress*, 518 (October): 71–82.
1419 <https://doi.org/10.1016/j.jhydrol.2014.01.018>.

1420 Wan Jaafar, Wan Zurina, and Dawei Han. 2012. "Uncertainty in Index Flood Modelling Due to
1421 Calibration Data Sizes." *Hydrological Processes* 26 (2): 189–201.
1422 <https://doi.org/10.1002/hyp.8135>.

1423 Wang, Jie, QiuHong Tang, Xiaobo Yun, Aifang Chen, Siao Sun, and Dai Yamazaki. 2022. "Flood
1424 Inundation in the Lancang Mekong River Basin: Assessing the Role of Summer
1425 Monsoon." *Journal of Hydrology* 612 (September): 128075.
1426 <https://doi.org/10.1016/j.jhydrol.2022.128075>.

1427 Wang, Zhaoli, Chengguang Lai, Xiaohong Chen, Bing Yang, Shiwei Zhao, and Xiaoyan Bai.
1428 2015. "Flood Hazard Risk Assessment Model Based on Random Forest." *Journal of
1429 Hydrology* 527 (August): 1130–41. <https://doi.org/10.1016/j.jhydrol.2015.06.008>.

1430 Wing, Oliver E. J., William Lehman, Paul D. Bates, Christopher C. Sampson, Niall Quinn, Andrew
1431 M. Smith, Jeffrey C. Neal, Jeremy R. Porter, and Carolyn Kousky. 2022. "Inequitable

1432 Patterns of US Flood Risk in the Anthropocene.” *Nature Climate Change* 12 (2): 156–62.
1433 <https://doi.org/10.1038/s41558-021-01265-6>.

1434 Youssef, Ahmed M., Biswajeet Pradhan, Abhirup Dikshit, and Ali M. Mahdi. 2022. “Comparative
1435 Study of Convolutional Neural Network (CNN) and Support Vector Machine (SVM) for
1436 Flood Susceptibility Mapping: A Case Study at Ras Gharib, Red Sea, Egypt.” *Geocarto
1437 International* 37 (26): 11088–115. <https://doi.org/10.1080/10106049.2022.2046866>.

1438 Zahura, Faria T., Jonathan L. Goodall, Jeffrey M. Sadler, Yawen Shen, Mohamed M. Morsy, and
1439 Madhur Behl. 2020. “Training Machine Learning Surrogate Models From a High Fidelity
1440 Physics Based Model: Application for Real Time Street Scale Flood Prediction in an
1441 Urban Coastal Community.” *Water Resources Research* 56 (10).
1442 <https://doi.org/10.1029/2019WR027038>.

1443 Zhang, Fang, Xiaolin Zhu, and Desheng Liu. 2014. “Blending MODIS and Landsat Images for
1444 Urban Flood Mapping.” *International Journal of Remote Sensing* 35 (9): 3237–53.
1445 <https://doi.org/10.1080/01431161.2014.903351>.

1446 Zhao, Gang, Bo Pang, Zongxue Xu, Lizhuang Cui, Jingjing Wang, Depeng Zuo, and Dingzhi
1447 Peng. 2021. “Improving Urban Flood Susceptibility Mapping Using Transfer Learning.”
1448 *Journal of Hydrology* 602 (November): 126777.
1449 <https://doi.org/10.1016/j.jhydrol.2021.126777>.

1450 Zhao, Gang, Bo Pang, Zongxue Xu, Dingzhi Peng, and Depeng Zuo. 2020. “Urban Flood
1451 Susceptibility Assessment Based on Convolutional Neural Networks.” *Journal of
1452 Hydrology* 590 (November): 125235. <https://doi.org/10.1016/j.jhydrol.2020.125235>.

1453 Zheng, Xing, David G. Tarboton, David R. Maidment, Yan Y. Liu, and Paola Passalacqua. 2018.
1454 “River Channel Geometry and Rating Curve Estimation Using Height above the Nearest

1455 Drainage.” *JAWRA Journal of the American Water Resources Association* 54 (4): 785–
1456 806. <https://doi.org/10.1111/1752-1688.12661>.

1457 Zhu, D., Q. Ren, Y. Xuan, Y. Chen, and I. D. Cluckie. 2013. “An Effective Depression Filling
1458 Algorithm for DEM Based 2-D Surface Flow Modelling.” *Hydrology and Earth System*
1459 *Sciences* 17 (2): 495–505. <https://doi.org/10.5194/hess-17-495-2013>.

1460 Zhu, Jun Jie, Meiqi Yang, and Zhiyong Jason Ren. 2023. “Machine Learning in Environmental
1461 Research: Common Pitfalls and Best Practices.” *Environmental Science & Technology*,
1462 June. <https://doi.org/10.1021/aes.est.3e00026>.

1463 Abdollahi, Abolfazl, and Biswajeet Pradhan. 2021. “Urban Vegetation Mapping from Aerial
1464 Imagery Using Explainable AI (XAI).” *Sensors* 21 (14): 4738.
1465 <https://doi.org/10.3390/s21144738>.

1466 Abdrabo, Karim I., Sameh A. Kantoush, Aly Esmail, Mohamed Saber, Tetsuya Sumi, Mahmood
1467 Almamari, Bahaa Elboshy, and Safaa Ghoniem. 2023. “An Integrated Indicator-Based
1468 Approach for Constructing an Urban Flood Vulnerability Index as an Urban Decision-
1469 Making Tool Using the PCA and AHP Techniques: A Case Study of Alexandria, Egypt.”
1470 *Urban Climate* 48 (March): 101426. <https://doi.org/10.1016/j.uclim.2023.101426>.

1471 Abrahart, Robert, P. E. Kneale, and Linda M. See. 2004. *Neural Networks for Hydrological*
1472 *Modeling*. CRC Press.

1473 Adamowski, Jan, Hiu Fung Chan, Shiv O. Prasher, and Vishwa Nath Sharda. 2011. “Comparison
1474 of Multivariate Adaptive Regression Splines with Coupled Wavelet Transform Artificial
1475 Neural Networks for Runoff Forecasting in Himalayan Micro-Watersheds with Limited
1476 Data.” *Journal of Hydroinformatics* 14 (3): 731–44.
1477 <https://doi.org/10.2166/hydro.2011.044>.

1478 Agarap, Abien Fred. 2019. “Deep Learning Using Rectified Linear Units (ReLU).” arXiv.
1479 <http://arxiv.org/abs/1803.08375>.

1480 Ahmadisharaf Ebrahim, Camacho René A., Zhang Harry X., Hantush Mohamed M., and
1481 Mohamoud Yusuf M. 2019. “Calibration and Validation of Watershed Models and
1482 Advances in Uncertainty Analysis in TMDL Studies.” *Journal of Hydrologic Engineering*
1483 24 (7): 03119001. [https://doi.org/10.1061/\(ASCE\)HE.1943-5584.0001794](https://doi.org/10.1061/(ASCE)HE.1943-5584.0001794).

1484 Ahmadisharaf, Ebrahim, and Alfred J Kalyanapu. 2019. “A Coupled Probabilistic Hydrologic and
1485 Hydraulic Modelling Framework to Investigate the Uncertainty of Flood Loss Estimates.”
1486 *Journal of Flood Risk Management* 12 (S2): e12536. <https://doi.org/10.1111/jfr3.12536>.

1487 Ahmadisharaf, Ebrahim, Alfred J. Kalyanapu, Jason R. Lillywhite, and Gina L. Tonn. 2018. “A
1488 Probabilistic Framework to Evaluate the Uncertainty of Design Hydrograph: Case Study
1489 of Swannanoa River Watershed.” *Hydrological Sciences Journal* 63 (12): 1776–90.
1490 <https://doi.org/10.1080/02626667.2018.1525616>.

- 1491 Allen, David M. 1974. "The Relationship Between Variable Selection and Data Augmentation and
1492 a Method for Prediction." Technometrics 16 (1): 125–27.
1493 <https://doi.org/10.1080/00401706.1974.10489157>.
- 1494 Anderson, Tiffany R., Charles H. Fletcher, Matthew M. Barbee, Bradley M. Romine, Sam Lemmo,
1495 and Jade M. S. Delevaux. 2018. "Modeling Multiple Sea Level Rise Stresses Reveals up
1496 to Twice the Land at Risk Compared to Strictly Passive Flooding Methods." Scientific
1497 Reports 8 (1): 14484. <https://doi.org/10.1038/s41598-018-32658-x>.
- 1498 Bafitlhile, Thabo Michael, and Zhijia Li. 2019. "Applicability of ϵ -Support Vector Machine and
1499 Artificial Neural Network for Flood Forecasting in Humid, Semi-Humid and Semi-Arid
1500 Basins in China." Water 11 (1): 85. <https://doi.org/10.3390/w11010085>.
- 1501 Bales, J.d., and C.r. Wagner. 2009. "Sources of Uncertainty in Flood Inundation Maps." Journal
1502 of Flood Risk Management 2 (2): 139–47. [https://doi.org/10.1111/j.1753-](https://doi.org/10.1111/j.1753-318X.2009.01029.x)
1503 [318X.2009.01029.x](https://doi.org/10.1111/j.1753-318X.2009.01029.x).
- 1504 Bates, Paul D. 2022. "Flood Inundation Prediction." Annual Review of Fluid Mechanics 54 (1):
1505 287–315. <https://doi.org/10.1146/annurev-fluid-030121-113138>.
- 1506 Bates, Paul D., Richard J. Dawson, Jim W. Hall, Matthew S. Horritt, Robert J. Nicholls, Jon Wicks,
1507 and Mohamed Ahmed Ali Mohamed Hassan. 2005. "Simplified Two-Dimensional
1508 Numerical Modelling of Coastal Flooding and Example Applications." Coastal
1509 Engineering 52 (9): 793–810. <https://doi.org/10.1016/j.coastaleng.2005.06.001>.
- 1510 Berkhahn, Simon, Lothar Fuchs, and Insa Neuweiler. 2019. "An Ensemble Neural Network Model
1511 for Real-Time Prediction of Urban Floods." Journal of Hydrology 575 (August): 743–54.
1512 <https://doi.org/10.1016/j.jhydrol.2019.05.066>.
- 1513 Beven II, John L., Andrew Hagen, and Robbie Berg. 2022. "Tropical Cyclone Report -
1514 HURRICANE IDA (AL092021)." National Hurricane Center. April 4, 2022.
1515 https://www.nhc.noaa.gov/data/tcr/AL092021_Ida.pdf.
- 1516 Beven, K. J., and M. J. Kirkby. 1979. "A Physically Based, Variable Contributing Area Model of
1517 Basin Hydrology / Un Modèle à Base Physique de Zone d'appel Variable de l'hydrologie
1518 Du Bassin Versant." Hydrological Sciences Bulletin 24 (1): 43–69.
1519 <https://doi.org/10.1080/02626667909491834>.
- 1520 Bhuyian, Md N. M., and Alfred Kalyanapu. 2020. "Predicting Channel Conveyance and
1521 Characterizing Planform Using River Bathymetry via Satellite Image Compilation
1522 (RiBaSIC) Algorithm for DEM-Based Hydrodynamic Modeling." Remote Sensing 12
1523 (17): 2799. <https://doi.org/10.3390/rs12172799>.
- 1524 Blake, Eric S., Todd B. Kimberlain, Robert J. Berg, John P. Cangialosi, and John L. Beven II.
1525 2013. "Tropical Cyclone Report - Hurricane Sandy (AL182012)." National Hurricane
1526 Center. February 12, 2013. https://www.nhc.noaa.gov/data/tcr/AL182012_Sandy.pdf.
- 1527 Bottou, Léon. 2012. "Stochastic Gradient Descent Tricks." In Neural Networks: Tricks of the
1528 Trade, edited by Grégoire Montavon, Geneviève B. Orr, and Klaus-Robert Müller,
1529 7700:421–36. Lecture Notes in Computer Science. Berlin, Heidelberg: Springer Berlin
1530 Heidelberg. https://doi.org/10.1007/978-3-642-35289-8_25.
- 1531 Cao, Yifan, Hongliang Jia, Junnan Xiong, Weiming Cheng, Kun Li, Quan Pang, and Zhiwei Yong.
1532 2020. "Flash Flood Susceptibility Assessment Based on Geodetector, Certainty Factor, and
1533 Logistic Regression Analyses in Fujian Province, China." ISPRS International Journal of
1534 Geo-Information 9 (12): 748. <https://doi.org/10.3390/ijgi9120748>.

1535 [Chang, Li-Chiu, Jia-Yi Liou, and Fi-John Chang. 2022. "Spatial-Temporal Flood Inundation](#)
1536 [Nowcasts by Fusing Machine Learning Methods and Principal Component Analysis."](#)
1537 [Journal of Hydrology](#) 612 (September): 128086.
1538 <https://doi.org/10.1016/j.jhydrol.2022.128086>.

1539 [Chen, Yuguo, Xinyi Zhang, Kejun Yang, Shiyi Zeng, and Anyu Hong. 2023. "Modeling Rules of](#)
1540 [Regional Flash Flood Susceptibility Prediction Using Different Machine Learning](#)
1541 [Models." Frontiers in Earth Science](#) 11.
1542 <https://www.frontiersin.org/articles/10.3389/feart.2023.1117004>.

1543 [Costabile, Pierfranco, Carmelina Costanzo, and Francesco Macchione. 2017. "Performances and](#)
1544 [Limitations of the Diffusive Approximation of the 2-d Shallow Water Equations for Flood](#)
1545 [Simulation in Urban and Rural Areas." Applied Numerical Mathematics, New Trends in](#)
1546 [Numerical Analysis: Theory, Methods, Algorithms and Applications \(NETNA 2015\), 116](#)
1547 [\(June\): 141–56. https://doi.org/10.1016/j.apnum.2016.07.003.](#)

1548 [Dawson, C. W., R. J. Abrahart, A. Y. Shamseldin, and R. L. Wilby. 2006. "Flood Estimation at](#)
1549 [Ungauged Sites Using Artificial Neural Networks." Journal of Hydrology](#) 319 (1): 391–

1550 [409. https://doi.org/10.1016/j.jhydrol.2005.07.032.](#)

1551 [Dixit, A, S Sahany, B Rajagopalan, and S Choubey. 2022. "Role of Changing Land Use and Land](#)
1552 [Cover \(LULC\) on the 2018 Megafloods over Kerala, India." Climate Research](#) 89
1553 [\(October\): 1–14. https://doi.org/10.3354/cr01701.](#)

1554 [Ebrahimian, Ali, Abdollah Ardeshtir, Iman Zahedi Rad, and Seyyed Hassan Ghodsypour. 2015.](#)
1555 ["Urban Stormwater Construction Method Selection Using a Hybrid Multi-Criteria](#)
1556 [Approach." Automation in Construction](#) 58 (October): 118–28.
1557 <https://doi.org/10.1016/j.autcon.2015.07.014>.

1558 [Ebrahimian, Ali, John S. Gulliver, and Bruce N. Wilson. 2016. "Effective Impervious Area for](#)
1559 [Runoff in Urban Watersheds: EIA in Urban Watersheds." Hydrological Processes](#) 30 (20):
1560 [3717–29. https://doi.org/10.1002/hyp.10839.](#)

1561 [Elkhrachy, Ismail. 2022. "Flash Flood Water Depth Estimation Using SAR Images, Digital](#)
1562 [Elevation Models, and Machine Learning Algorithms." Remote Sensing](#) 14 (3): 440.
1563 <https://doi.org/10.3390/rs14030440>.

1564 [Fereshtehpour, Mohammad, Mostafa Esmailzadeh, Reza Saleh Alipour, and Steven J. Burian.](#)
1565 [2024. "Impacts of DEM Type and Resolution on Deep Learning-Based Flood Inundation](#)
1566 [Mapping." Earth Science Informatics](#) 17 (2): 1125–45. [https://doi.org/10.1007/s12145-](https://doi.org/10.1007/s12145-024-01239-0)
1567 [024-01239-0.](#)

1568 [Fernández-Pato, Javier, Daniel Caviedes-Voullième, and Pilar García-Navarro. 2016.](#)
1569 ["Rainfall/Runoff Simulation with 2D Full Shallow Water Equations: Sensitivity Analysis](#)
1570 [and Calibration of Infiltration Parameters." Journal of Hydrology](#) 536 (May): 496–513.
1571 <https://doi.org/10.1016/j.jhydrol.2016.03.021>.

1572 [Gallegos, Humberto A., Jochen E. Schubert, and Brett F. Sanders. 2012. "Structural Damage](#)
1573 [Prediction in a High-Velocity Urban Dam-Break Flood: Field-Scale Assessment of](#)
1574 [Predictive Skill." Journal of Engineering Mechanics](#) 138 (10): 1249–62.
1575 [https://doi.org/10.1061/\(ASCE\)EM.1943-7889.0000427](https://doi.org/10.1061/(ASCE)EM.1943-7889.0000427).

1576 [Geisser, Seymour. 1975. "The Predictive Sample Reuse Method with Applications." Journal of](#)
1577 [the American Statistical Association](#) 70 (350): 320–28.
1578 <https://doi.org/10.1080/01621459.1975.10479865>.

1579 Gray W. Brunner. 2016. "HEC-RAS, River Analysis System Hydraulic Reference Manual."
1580 February 2016. [https://www.hec.usace.army.mil/software/hec-ras/documentation/HEC-](https://www.hec.usace.army.mil/software/hec-ras/documentation/HEC-RAS%205.0%20Reference%20Manual.pdf)
1581 [RAS%205.0%20Reference%20Manual.pdf](https://www.hec.usace.army.mil/software/hec-ras/documentation/HEC-RAS%205.0%20Reference%20Manual.pdf).
1582 Gudiyangada Nachappa, Thimmaiah, Sepideh Tavakkoli Piralilou, Khalil Gholamnia, Omid
1583 Ghorbanzadeh, Omid Rahmati, and Thomas Blaschke. 2020. "Flood Susceptibility
1584 Mapping with Machine Learning, Multi-Criteria Decision Analysis and Ensemble Using
1585 Dempster Shafer Theory." *Journal of Hydrology* 590 (November): 125275.
1586 <https://doi.org/10.1016/j.jhydrol.2020.125275>.
1587 Guo, Zifeng, João P. Leitão, Nuno E. Simões, and Vahid Moosavi. 2021. "Data-Driven Flood
1588 Emulation: Speeding up Urban Flood Predictions by Deep Convolutional Neural
1589 Networks." *Journal of Flood Risk Management* 14 (1): e12684.
1590 <https://doi.org/10.1111/jfr3.12684>.
1591 Horel, Enguerrand, and Kay Giesecke. 2019. "Computationally Efficient Feature Significance and
1592 Importance for Machine Learning Models." <https://doi.org/10.48550/ARXIV.1905.09849>.
1593 Hosseini, Farzaneh Sajedi, Bahram Choubin, Amir Mosavi, Narjes Nabipour, Shahaboddin
1594 Shamshirband, Hamid Darabi, and Ali Torabi Haghighi. 2020. "Flash-Flood Hazard
1595 Assessment Using Ensembles and Bayesian-Based Machine Learning Models: Application
1596 of the Simulated Annealing Feature Selection Method." *Science of The Total Environment*
1597 711 (April): 135161. <https://doi.org/10.1016/j.scitotenv.2019.135161>.
1598 Hosseiny, Hossein, Foad Nazari, Virginia Smith, and C. Nataraj. 2020. "A Framework for
1599 Modeling Flood Depth Using a Hybrid of Hydraulics and Machine Learning." *Scientific*
1600 *Reports* 10 (1): 8222. <https://doi.org/10.1038/s41598-020-65232-5>.
1601 Hu, Anson, and Ibrahim Demir. 2021. "Real-Time Flood Mapping on Client-Side Web Systems
1602 Using HAND Model." *Hydrology* 8 (2): 65. <https://doi.org/10.3390/hydrology8020065>.
1603 Huang, Faming, Siyu Tao, Deying Li, Zhipeng Lian, Filippo Catani, Jinsong Huang, Kailong Li,
1604 and Chuhong Zhang. 2022. "Landslide Susceptibility Prediction Considering
1605 Neighborhood Characteristics of Landslide Spatial Datasets and Hydrological Slope Units
1606 Using Remote Sensing and GIS Technologies." *Remote Sensing* 14 (18): 4436.
1607 <https://doi.org/10.3390/rs14184436>.
1608 Jafarzagadean, Keighobad, and Venkatesh Merwade. 2019. "Probabilistic Floodplain Mapping
1609 Using HAND-Based Statistical Approach." *Geomorphology* 324 (January): 48–61.
1610 <https://doi.org/10.1016/j.geomorph.2018.09.024>.
1611 Jafarzagadean, Keighobad, Hamid Moradkhani, Florian Pappenberger, Hamed Moftakhari, Paul
1612 Bates, Peyman Abbaszadeh, Reza Marsooli, et al. 2023. "Recent Advances and New
1613 Frontiers in Riverine and Coastal Flood Modeling." *Reviews of Geophysics* 61 (2):
1614 e2022RG000788. <https://doi.org/10.1029/2022RG000788>.
1615 Jiang, Junguang, Yang Shu, Jianmin Wang, and Mingsheng Long. 2024. "Transferability in Deep
1616 Learning: A Survey." *Arxiv*. 2024. <https://arxiv.labs.arxiv.org/html/2201.05867>.
1617 Joseph, V. Roshan. 2022. "Optimal Ratio for Data Splitting." *Statistical Analysis and Data Mining:*
1618 *The ASA Data Science Journal* 15 (4): 531–38. <https://doi.org/10.1002/sam.11583>.
1619 Kalyanapu, Alfred J., Siddharth Shankar, Eric R. Pardyjak, David R. Judi, and Steven J. Burian.
1620 2011. "Assessment of GPU Computational Enhancement to a 2D Flood Model." *Environmental*
1621 *Modelling & Software* 26 (8): 1009–16.
1622 <https://doi.org/10.1016/j.envsoft.2011.02.014>.

1623 [Karamouz, Mohammad, Reza Saleh Alipour, Mahnoor Roohinia, and Mohammad Fereshtehpour. 2022. "A Remote Sensing Driven Soil Moisture Estimator: Uncertain Downscaling With Geostatistically Based Use of Ancillary Data." *Water Resources Research* 58 \(10\): e2022WR031946. <https://doi.org/10.1029/2022WR031946>.](#)

1624

1625 [Khosravi, Khabat, Binh Thai Pham, Kamran Chapi, Ataollah Shirzadi, Himan Shahabi, Inge Revhaug, Indra Prakash, and Dieu Tien Bui. 2018. "A Comparative Assessment of Decision Trees Algorithms for Flash Flood Susceptibility Modeling at Haraz Watershed, Northern Iran." *Science of The Total Environment* 627 \(June\): 744–55. <https://doi.org/10.1016/j.scitotenv.2018.01.266>.](#)

1626

1627

1628 [Kim, Sooyoul, Yoshiharu Matsumi, Shunqi Pan, and Hajime Mase. 2016. "A Real-Time Forecast Model Using Artificial Neural Network for after-Runner Storm Surges on the Tottori Coast, Japan." *Ocean Engineering* 122 \(August\): 44–53. <https://doi.org/10.1016/j.oceaneng.2016.06.017>.](#)

1629

1630

1631 [Kreibich, H., K. Piroth, I. Seifert, H. Maiwald, U. Kunert, J. Schwarz, B. Merz, and A. H. Thieken. 2009. "Is Flow Velocity a Significant Parameter in Flood Damage Modelling?" *Natural Hazards and Earth System Sciences* 9 \(5\): 1679–92. <https://doi.org/10.5194/nhess-9-1679-2009>.](#)

1632

1633

1634 [Kulp, Scott A., and Benjamin H. Strauss. 2019. "New Elevation Data Triple Estimates of Global Vulnerability to Sea-Level Rise and Coastal Flooding." *Nature Communications* 10 \(1\): 4844. <https://doi.org/10.1038/s41467-019-12808-z>.](#)

1635

1636 [Kundzewicz, ZW, Buda Su, Yanjun Wang, Jun Xia, Jinlong Huang, and Tong Jiang. 2019. "Flood Risk and Its Reduction in China." *Advances in Water Resources* 130 \(August\): 37–45. <https://doi.org/10.1016/j.advwatres.2019.05.020>.](#)

1637

1638 [Latto, Andy, Andrew Hagen, and Robbie Berg. 2021. "Tropical Cyclone Report - HURRICANE ISAIAS \(AL092020\)." National Hurricane Center. June 11, 2021. \[https://www.nhc.noaa.gov/data/tcr/AL092020_Isaias.pdf\]\(https://www.nhc.noaa.gov/data/tcr/AL092020_Isaias.pdf\).](#)

1639

1640 [Lee, Deuk-Hwan, Yun-Tae Kim, and Seung-Rae Lee. 2020. "Shallow Landslide Susceptibility Models Based on Artificial Neural Networks Considering the Factor Selection Method and Various Non-Linear Activation Functions." *Remote Sensing* 12 \(7\): 1194. <https://doi.org/10.3390/rs12071194>.](#)

1641

1642 [Lixion A., Avila, and John Cangialosi. 2013. "Tropical Cyclone Report - Hurricane Irene \(AL092011\)." National Hurricane Center. April 11, 2013. \[https://www.nhc.noaa.gov/data/tcr/AL092011_Irene.pdf\]\(https://www.nhc.noaa.gov/data/tcr/AL092011_Irene.pdf\).](#)

1643

1644 [Löwe, Roland, Julian Böhm, David Getreuer Jensen, Jorge Leandro, and Søren Højmark Rasmussen. 2021. "U-FLOOD – Topographic Deep Learning for Predicting Urban Pluvial Flood Water Depth." *Journal of Hydrology* 603 \(December\): 126898. <https://doi.org/10.1016/j.jhydrol.2021.126898>.](#)

1645

1646 [Lundberg, Scott, and Su-In Lee. 2017. "A Unified Approach to Interpreting Model Predictions." *arXiv*. <http://arxiv.org/abs/1705.07874>.](#)

1647

1648 [Macedo, Francisco, M. Rosário Oliveira, António Pacheco, and Rui Valadas. 2019. "Theoretical Foundations of Forward Feature Selection Methods Based on Mutual Information." *Neurocomputing* 325 \(January\): 67–89. <https://doi.org/10.1016/j.neucom.2018.09.077>.](#)

1649

1650 [McCulloch, Warren S., and Walter Pitts. 1943. "A Logical Calculus of the Ideas Immanent in Nervous Activity." *The Bulletin of Mathematical Biophysics* 5 \(4\): 115–33. <https://doi.org/10.1007/BF02478259>.](#)

1651

1652

1653

1654

1655

1656

1657

1668 [Merwade, Venkatesh, Francisco Olivera, Mazdak Arabi, and Scott Edleman. 2008. "Uncertainty](#)
1669 [in Flood Inundation Mapping: Current Issues and Future Directions." Journal of](#)
1670 [Hydrologic Engineering 13 \(7\): 608–20. \[0699\\(2008\\)13:7\\(608\\).\]\(https://doi.org/10.1061/\(ASCE\)1084-

1671 <a href=\)](#)

1672 [Merz, B, Heidi Kreibich, R Schwarze, and Annette Thielen. 2010. "Review Article" Assessment](#)
1673 [of Economic Flood Damage". Natural Hazards and Earth System Sciences 10: 1697–](#)
1674 [1724. <https://doi.org/10.5194/nhess-10-1697-2010>.](#)

1675 [Ming, Xiaodong, Qiuhua Liang, Xilin Xia, Dingmin Li, and Hayley J. Fowler. 2020. "Real-Time](#)
1676 [Flood Forecasting Based on a High-Performance 2-D Hydrodynamic Model and](#)
1677 [Numerical Weather Predictions." Water Resources Research 56 \(7\): e2019WR025583.](#)
1678 [https://doi.org/10.1029/2019WR025583.](#)

1679 [Mishra, Ashok, Sourav Mukherjee, Bruno Merz, Vijay P. Singh, Daniel B. Wright, Villarini](#)
1680 [Gabriele, Subir Paul, et al. 2022. "An Overview of Flood Concepts, Challenges, and Future](#)
1681 [Directions." Journal of Hydrologic Engineering 27 \(6\).](#)
1682 [https://ascelibrary.org/doi/full/10.1061/\(ASCE\)HE.1943-5584.0002164.](#)

1683 [National Hurricane Center. 2022. "National Hurricane Center." 2022.](#)
1684 [https://www.nhc.noaa.gov/index.shtml.](#)

1685 [Nguyen, Quang Hung, Hai-Bang Ly, Lanh Si Ho, Nadhir Al-Ansari, Hiep Van Le, Van Quan Tran,](#)
1686 [Indra Prakash, and Binh Thai Pham. 2021. "Influence of Data Splitting on Performance of](#)
1687 [Machine Learning Models in Prediction of Shear Strength of Soil." Mathematical Problems](#)
1688 [in Engineering 2021 \(February\): e4832864. <https://doi.org/10.1155/2021/4832864>.](#)

1689 [NOAA. 2023. "NOAA Tides & Currents." CO-OPS Map - NOAA Tides & Currents. 2023.](#)
1690 [https://tidesandcurrents.noaa.gov/map/index.html.](#)

1691 [NOAA's NCEI. 2022. "Data Search | National Centers for Environmental Information \(NCEI\)." 2022.](#)
1692 [https://www.ncei.noaa.gov/access/search/data-search/local-climatological-data.](#)

1693 [Park, Man Ho, Munsol Ju, and Jae Young Kim. 2020. "Bayesian Approach in Estimating Flood](#)
1694 [Waste Generation: A Case Study in South Korea." Journal of Environmental Management](#)
1695 [265 \(July\): 110552. <https://doi.org/10.1016/j.jenvman.2020.110552>.](#)

1696 [Pham, Binh Thai, Chinh Luu, Tran Van Phong, Phan Trong Trinh, Ataollah Shirzadi, Somayeh](#)
1697 [Renoud, Shahrokh Asadi, Hiep Van Le, Jason von Meding, and John J. Clague. 2021. "Can](#)
1698 [Deep Learning Algorithms Outperform Benchmark Machine Learning Algorithms in](#)
1699 [Flood Susceptibility Modeling?" Journal of Hydrology 592 \(January\): 125615.](#)
1700 [https://doi.org/10.1016/j.jhydrol.2020.125615.](#)

1701 [Pradhan, Biswajeet. 2009. "Journal of Spatial Hydrology Vol.9, No.2 Fall 2009."](#)

1702 [Qi, Honghai, and Mustafa S. Altinakar. 2011a. "A Conceptual Framework of Agricultural Land](#)
1703 [Use Planning with BMP for Integrated Watershed Management." Journal of](#)
1704 [Environmental Management 92 \(1\): 149–55.](#)
1705 [https://doi.org/10.1016/j.jenvman.2010.08.023.](#)

1706 [———. 2011b. "Vegetation Buffer Strips Design Using an Optimization Approach for Non-Point](#)
1707 [Source Pollutant Control of an Agricultural Watershed." Water Resources Management 25](#)
1708 [\(2\): 565–78. <https://doi.org/10.1007/s11269-010-9714-9>.](#)

1709 [———. 2012. "GIS-Based Decision Support System for Dam Break Flood Management under](#)
1710 [Uncertainty with Two-Dimensional Numerical Simulations." Journal of Water Resources](#)
1711 [Planning and Management 138 \(4\): 334–41. \[5452.0000192.\]\(https://doi.org/10.1061/\(ASCE\)WR.1943-

1712 <a href=\)](#)

- 1713 [Rafiei-Sardooi, Elham, Ali Azareh, Bahram Choubin, Amir H. Mosavi, and John J. Clague. 2021.](#)
1714 [“Evaluating Urban Flood Risk Using Hybrid Method of TOPSIS and Machine Learning.”](#)
1715 [International Journal of Disaster Risk Reduction 66 \(December\): 102614.](#)
1716 [https://doi.org/10.1016/j.ijdrr.2021.102614.](https://doi.org/10.1016/j.ijdrr.2021.102614)
- 1717 [Rahmati, Omid, Hamid Reza Pourghasemi, and Hossein Zeinivand. 2016. “Flood Susceptibility](#)
1718 [Mapping Using Frequency Ratio and Weights-of-Evidence Models in the Golastan](#)
1719 [Province, Iran.” Geocarto International 31 \(1\): 42–70.](#)
1720 [https://doi.org/10.1080/10106049.2015.1041559.](https://doi.org/10.1080/10106049.2015.1041559)
- 1721 [Reckien, Diana. 2018. “What Is in an Index? Construction Method, Data Metric, and Weighting](#)
1722 [Scheme Determine the Outcome of Composite Social Vulnerability Indices in New York](#)
1723 [City.” Regional Environmental Change 18 \(5\): 1439–51. https://doi.org/10.1007/s10113-](#)
1724 [017-1273-7.](#)
- 1725 [Rennó, Camilo Daleles, Antonio Donato Nobre, Luz Adriana Cuartas, João Vianei Soares, Martin](#)
1726 [G. Hodnett, Javier Tomasella, and Maarten J. Waterloo. 2008. “HAND, a New Terrain](#)
1727 [Descriptor Using SRTM-DEM: Mapping Terra-Firme Rainforest Environments in](#)
1728 [Amazonia.” Remote Sensing of Environment 112 \(9\): 3469–81.](#)
1729 [https://doi.org/10.1016/j.rse.2008.03.018.](https://doi.org/10.1016/j.rse.2008.03.018)
- 1730 [Rezaei, Fatemeh, Mahdi Panahi, Sayed M. Bateni, Changyun Jun, Christopher M. U. Neale, and](#)
1731 [Saro Lee. 2022. “Novel Hybrid Models by Coupling Support Vector Regression \(SVR\)](#)
1732 [with Meta-Heuristic Algorithms \(WOA and GWO\) for Flood Susceptibility Mapping.”](#)
1733 [Natural Hazards 114 \(2\): 1247–83. https://doi.org/10.1007/s11069-022-05424-6.](#)
- 1734 [Rumelhart, David E., James L. McClelland, and PDP Research Group. 1986. Parallel Distributed](#)
1735 [Processing: Explorations in the Microstructure of Cognition: Foundations. The MIT Press.](#)
1736 [https://doi.org/10.7551/mitpress/5236.001.0001.](https://doi.org/10.7551/mitpress/5236.001.0001)
- 1737 [Salvati, Aryan, Alireza Moghaddam Nia, Ali Salajegheh, Kayvan Ghaderi, Dawood Talebpour](#)
1738 [Asl, Nadhir Al-Ansari, Feridon Solaimani, and John J. Clague. 2023. “Flood Susceptibility](#)
1739 [Mapping Using Support Vector Regression and Hyper-Parameter Optimization.” Journal](#)
1740 [of Flood Risk Management n/a \(n/a\): e12920. https://doi.org/10.1111/jfr3.12920.](#)
- 1741 [Schubert, Jochen E., Adam Luke, Amir AghaKouchak, and Brett F. Sanders. 2022. “A Framework](#)
1742 [for Mechanistic Flood Inundation Forecasting at the Metropolitan Scale.” Water Resources](#)
1743 [Research 58 \(10\): e2021WR031279. https://doi.org/10.1029/2021WR031279.](#)
- 1744 [Schubert, Jochen E., and Brett F. Sanders. 2012. “Building Treatments for Urban Flood Inundation](#)
1745 [Models and Implications for Predictive Skill and Modeling Efficiency.” Advances in Water](#)
1746 [Resources 41 \(June\): 49–64. https://doi.org/10.1016/j.advwatres.2012.02.012.](#)
- 1747 [Sheridan, Scott C., Cameron C. Lee, Ryan E. Adams, Erik T. Smith, Douglas E. Pirhalla, and Varis](#)
1748 [Ransibrahmanakul. 2019. “Temporal Modeling of Anomalous Coastal Sea Level Values](#)
1749 [Using Synoptic Climatological Patterns.” Journal of Geophysical Research: Oceans 124](#)
1750 [\(9\): 6531–44. https://doi.org/10.1029/2019JC015421.](#)
- 1751 [Singarimbun, Roy Nuary, Erna Budhiarti Nababan, and Opim Salim Sitompul. 2019. “Adaptive](#)
1752 [Moment Estimation To Minimize Square Error In Backpropagation Algorithm.” In 2019](#)
1753 [International Conference of Computer Science and Information Technology](#)
1754 [\(ICoSNIKOM\), 1–7. Medan, Indonesia: IEEE.](#)
1755 [https://doi.org/10.1109/ICoSNIKOM48755.2019.9111563.](https://doi.org/10.1109/ICoSNIKOM48755.2019.9111563)

1756 [Sridhar, Venkataramana, Syed Azhar Ali, and David J. Sample. 2021. "Systems Analysis of](#)
1757 [Coupled Natural and Human Processes in the Mekong River Basin." *Hydrology* 8 \(3\): 140.](#)
1758 [https://doi.org/10.3390/hydrology8030140.](https://doi.org/10.3390/hydrology8030140)

1759 [Stone, M. 1974. "Cross-Validatory Choice and Assessment of Statistical Predictions." *Journal of*](#)
1760 [the Royal Statistical Society: Series B \(Methodological\) 36 \(2\): 111–33.](#)
1761 [https://doi.org/10.1111/j.2517-6161.1974.tb00994.x.](https://doi.org/10.1111/j.2517-6161.1974.tb00994.x)

1762 [Stow, Craig A., Chris Roessler, Mark E. Borsuk, James D. Bowen, and Kenneth H. Reckhow.](#)
1763 [2003. "Comparison of Estuarine Water Quality Models for Total Maximum Daily Load](#)
1764 [Development in Neuse River Estuary." *Journal of Water Resources Planning and*](#)
1765 [Management 129 \(4\): 307–14. \[https://doi.org/10.1061/\\(ASCE\\)0733-\]\(https://doi.org/10.1061/\(ASCE\)0733-9496\(2003\)129:4\(307\)\)](#)
1766 [9496\(2003\)129:4\(307\).](https://doi.org/10.1061/(ASCE)0733-9496(2003)129:4(307))

1767 [Sun, Deliang, Jiahui Xu, Haijia Wen, and Yue Wang. 2020. "An Optimized Random Forest Model](#)
1768 [and Its Generalization Ability in Landslide Susceptibility Mapping: Application in Two](#)
1769 [Areas of Three Gorges Reservoir, China." *Journal of Earth Science* 31 \(6\): 1068–86.](#)
1770 [https://doi.org/10.1007/s12583-020-1072-9.](https://doi.org/10.1007/s12583-020-1072-9)

1771 [Teng, J., A.J. Jakeman, J. Vaze, B.F.W. Croke, D. Dutta, and S. Kim. 2017. "Flood Inundation](#)
1772 [Modelling: A Review of Methods, Recent Advances and Uncertainty Analysis." *Environmental*](#)
1773 [Modelling & Software 90 \(April\): 201–16.](#)
1774 [https://doi.org/10.1016/j.envsoft.2017.01.006.](https://doi.org/10.1016/j.envsoft.2017.01.006)

1775 [Trottier, Ludovic, Philippe Giguere, and Brahim Chaib-draa. 2017. "Parametric Exponential](#)
1776 [Linear Unit for Deep Convolutional Neural Networks." In *2017 16th IEEE International*](#)
1777 [Conference on Machine Learning and Applications \(ICMLA\), 207–14. Cancun, Mexico:](#)
1778 [IEEE. \[https://doi.org/10.1109/ICMLA.2017.00038.\]\(https://doi.org/10.1109/ICMLA.2017.00038\)](#)

1779 [USGS. 2022. "TNM Download V2." 2022. \[https://apps.nationalmap.gov/downloader/.\]\(https://apps.nationalmap.gov/downloader/\)](#)

1780 [Viglione, Alberto, Giuliano Di Baldassarre, Luigia Brandimarte, Linda Kuil, Gemma Carr, José](#)
1781 [Luis Salinas, Anna Scolobig, and Günter Blöschl. 2014. "Insights from Socio-Hydrology](#)
1782 [Modelling on Dealing with Flood Risk – Roles of Collective Memory, Risk-Taking](#)
1783 [Attitude and Trust." *Journal of Hydrology, Creating Partnerships Between Hydrology and*](#)
1784 [Social Science: A Priority for Progress, 518 \(October\): 71–82.](#)
1785 [https://doi.org/10.1016/j.jhydrol.2014.01.018.](https://doi.org/10.1016/j.jhydrol.2014.01.018)

1786 [Wagenaar, Dennis, Stefan Lüdtkke, Kai Schröter, Laurens M. Bouwer, and Heidi Kreibich. 2018.](#)
1787 ["Regional and Temporal Transferability of Multivariable Flood Damage Models." *Water*](#)
1788 [Resources Research 54 \(5\): 3688–3703. \[https://doi.org/10.1029/2017WR022233.\]\(https://doi.org/10.1029/2017WR022233\)](#)

1789 [Wan Jaafar, Wan Zurina, and Dawei Han. 2012. "Uncertainty in Index Flood Modelling Due to](#)
1790 [Calibration Data Sizes." *Hydrological Processes* 26 \(2\): 189–201.](#)
1791 [https://doi.org/10.1002/hyp.8135.](https://doi.org/10.1002/hyp.8135)

1792 [Wang, Jie, QiuHong Tang, Xiaobo Yun, Aifang Chen, Siao Sun, and Dai Yamazaki. 2022. "Flood](#)
1793 [Inundation in the Lancang-Mekong River Basin: Assessing the Role of Summer](#)
1794 [Monsoon." *Journal of Hydrology* 612 \(September\): 128075.](#)
1795 [https://doi.org/10.1016/j.jhydrol.2022.128075.](https://doi.org/10.1016/j.jhydrol.2022.128075)

1796 [Wang, Zhaoli, Chengguang Lai, Xiaohong Chen, Bing Yang, Shiwei Zhao, and Xiaoyan Bai.](#)
1797 [2015. "Flood Hazard Risk Assessment Model Based on Random Forest." *Journal of*](#)
1798 [Hydrology 527 \(August\): 1130–41. \[https://doi.org/10.1016/j.jhydrol.2015.06.008.\]\(https://doi.org/10.1016/j.jhydrol.2015.06.008\)](#)

1799 Wenger, Seth J., and Julian D. Olden. 2012. "Assessing Transferability of Ecological Models: An
1800 Underappreciated Aspect of Statistical Validation." *Methods in Ecology and Evolution* 3
1801 (2): 260–67. <https://doi.org/10.1111/j.2041-210X.2011.00170.x>.
1802 Youssef, Ahmed M., Biswajeet Pradhan, Abhirup Dikshit, and Ali M. Mahdi. 2022. "Comparative
1803 Study of Convolutional Neural Network (CNN) and Support Vector Machine (SVM) for
1804 Flood Susceptibility Mapping: A Case Study at Ras Gharib, Red Sea, Egypt." *Geocarto*
1805 *International* 37 (26): 11088–115. <https://doi.org/10.1080/10106049.2022.2046866>.
1806 Zahura, Faria T., Jonathan L. Goodall, Jeffrey M. Sadler, Yawen Shen, Mohamed M. Morsy, and
1807 Madhur Behl. 2020. "Training Machine Learning Surrogate Models From a High-Fidelity
1808 Physics-Based Model: Application for Real-Time Street-Scale Flood Prediction in an
1809 Urban Coastal Community." *Water Resources Research* 56 (10).
1810 <https://doi.org/10.1029/2019WR027038>.
1811 Zhang, Fang, Xiaolin Zhu, and Desheng Liu. 2014. "Blending MODIS and Landsat Images for
1812 Urban Flood Mapping." *International Journal of Remote Sensing* 35 (9): 3237–53.
1813 <https://doi.org/10.1080/01431161.2014.903351>.
1814 Zhao, Gang, Bo Pang, Zongxue Xu, Dingzhi Peng, and Depeng Zuo. 2020. "Urban Flood
1815 Susceptibility Assessment Based on Convolutional Neural Networks." *Journal of*
1816 *Hydrology* 590 (November): 125235. <https://doi.org/10.1016/j.jhydrol.2020.125235>.
1817 Zheng, Xing, David G. Tarboton, David R. Maidment, Yan Y. Liu, and Paola Passalacqua. 2018.
1818 "River Channel Geometry and Rating Curve Estimation Using Height above the Nearest
1819 Drainage." *JAWRA Journal of the American Water Resources Association* 54 (4): 785–
1820 806. <https://doi.org/10.1111/1752-1688.12661>.
1821 Zhu, D., Q. Ren, Y. Xuan, Y. Chen, and I. D. Cluckie. 2013. "An Effective Depression Filling
1822 Algorithm for DEM-Based 2-D Surface Flow Modelling." *Hydrology and Earth System*
1823 *Sciences* 17 (2): 495–505. <https://doi.org/10.5194/hess-17-495-2013>.
1824 Zhu, Jun-Jie, Meiqi Yang, and Zhiyong Jason Ren. 2023. "Machine Learning in Environmental
1825 Research: Common Pitfalls and Best Practices." *Environmental Science & Technology*,
1826 June. <https://doi.org/10.1021/acs.est.3c00026>.
1827

Formatted: Left, Line spacing: single